HELSINGIN YLIOPISTO
HELSINGFORS UNIVERSITET
UNIVERSITY OF HELSINKI

Master`s thesis

Petrology and Economic Geology

FACTOR ANALYSIS OF A LARGE GEOCHEMICAL EXPLORATION DATA SET – EXAMPLE FROM KALBA GOLD BELT, EASTERN KAZAKHSTAN

Juuso Uusikorpi

03/2020

Supervisor: Petri Peltonen

UNIVERSITY OF HELSINKI
FACULTY OF SCIENCE
DEPARTMENT OF GEOSCIENCES AND GEOGRAPHY

PL 64 (Gustaf Hällströmin katu 2)
00014 Helsingin yliopisto

HELSINGIN YLIOPISTO
HELSINGFORS UNIVERSITET
UNIVERSITY OF HELSINKI

Tiedekunta/Osasto Fakultet/Sektion – Faculty Faculty of Science	Koulutusohjelma/Utbildningsprogram – Degree programme Master's programme in Geology and Geophysics	
Tekijä/Författare – Author Juuso Jeremias Uusikorpi		
Työn nimi / Arbetets titel – Title Factor analysis of large geochemical exploration data set – example from Kalba gold belt, eastern Kazakhstan		
Opintosuunta/ Studieinriktning – Study track Petrology and Economic Geology		
Työn laji/Arbetets art – Level Master's thesis	Aika/Datum – Month and year 03/2020	Sivumäärä/ Sidoantal – Number of pages 69

Tiivistelmä/Referat – Abstract

The geochemical regolith data gathered from Dzhumba, a gold prospect in eastern Kazakhstan, was analyzed using factor analysis and then integrated into ArcGIS as spatial data. Principal axis factoring method was used for factor extraction combined with varimax orthogonal rotation and Kaiser normalization. Five clear factors were extracted from the data set of 47 elements in 3942 regolith samples. Kriging interpolation was used to generate spatial data surfaces from factor scores. The generated factors are composed of the geochemical associations in the raw data, and represent the underlying geological processes and formations of the area.

The fourth factor generated represents gold mineralization with As, Sb, Au, Zr, Sc, Mn, Mo, Cu, K and Ni being the elements that are positively loaded onto factor 4. Therefore, single element maps of these elements have been produced alongside the factor maps in order to examine factor 4 more intensely. Also maps about structural geology and alteration in the Dzhumba project area have been produced in order to give better understanding of the factor maps. The data suggests that the deposit type is an orogenic gold deposit.

Other factors created interesting results as well, and they gave information about the different geological units of the area. Factor 1 represents granitic rocks by their feldspar and trace element content, factor 2 represents black shales with possible mafic rock constituents, factor 3 represents a sulfide rich mafic mineral group or graphitic rocks that are most likely black shales and factor 5 possibly represents calcite alteration.

Factor 4 is the main interest of this study. The most intense loadings for factor 4 are in Brigadnoe, Svistun and Dzhumba with a small peak in Belyi. Single element map for gold mostly corresponds to factor 4 for Svistun and Dzhumba, but Brigadnoe is represented with a small peak. However, gold has a major presence in Fedor-Ivanovskoe, which is absent from factor 4.

Further exploration in Fedor-Ivanovskoe could be performed in order to clarify if this is due to an unrelated gold-only deposit or some other event. Possible future exploration in the area could benefit from factor 4 results, using As and Sb, or a combination of As, Sb, Zr, Sc, Mn, Mo, Cu, K and Ni as pathfinders for possible gold occurrences.

Avainsanat – Nyckelord – Keywords
Factor analysis, Gold exploration, Western Kalba belt, Eastern Kazakhstan, Geochemical exploration

Säilytyspaikka – Förvaringställe – Where deposited
HELDA – Digital repository of University of Helsinki

Muita tietoja – Övriga uppgifter – Additional information
24 figures and 9 tables

TABLE OF CONTENTS

1. INTRODUCTION

1.1. Gold in eastern Kazakhstan

Gold is a high value commodity that is actively explored in almost every country in the world. Kazakhstan is one of the more prospective countries that has a rising industrial mining sector and high potential for discovery of new gold deposits. One especially interesting area is located in eastern Kazakhstan, where the western Kalba gold-bearing belt already hosts 450 gold occurrence deposits and is therefore an extremely interesting location for gold exploration (Dyachkov et al., 2018; Kovalev et al., 2009). One of the most famous deposit in the western Kalba belt is the Bakyrchik gold mine, where open pit production commenced in 1956. The ore is disseminated gold-bearing sulfides in a black shale formation with gold reserves of 8.5 Moz (Polymetalinternational, 2020).

This thesis focuses on the eastern flank of the western Kalba belt, on a project area named Dzhumba. Gold occurrence in Dzhumba has been known since from the 1910's and high-grade veins of Au up to 200 ppm have been selectively mined from 1913 to 1955 (Kirmasov et al., 2017). Open pit mining operated from 1977 to 1981 (average grade of 5 ppm Au) and underground mining down to a depth of 150 meters was active from 1988 to 1990 (average grade of 30 ppm Au). Previous studies in Dzhumba have included geochemical surveys, magnetic surveys, an IP survey and trenching (Kirmasov et al., 2017).

1.2. Aim of this study

The purpose of this thesis is to use multivariate analysis, namely factor analysis to discover hard to distinguish correlations between gold and other elements for the benefit of exploration. Nearly 4000 samples have been collected from Dzhumba gold prospect area (Figure 1.), and the chemical composition of each sample has been analyzed. The data was collected during the exploration campaign of Kazzinc – the Kazakhstan state owned exploration and mining company. Due to the large number of samples and each

sample containing analyses of more than 20 elements, multivariate analysis is a suitable tool to examine correlations between the elements. Where regular correlation analysis shows the correlation between element pairs, factor analysis places the elements into groups of multiple elements that represent similar behavior (Tripathi, 1979). Analyzing the samples using multivariate analysis should give new perspective to the target area, and instead of having a different abundance map for every single element, produce a couple of maps showing grouped gold related elements. Better understanding of elemental relationships may help to develop new geochemical exploration tools for the region. The hypothesis is that factor analysis will reveal a factor that is clearly a gold mineralization composed of Au and its pathfinder elements, such as S, Mo, W, As, Zn, Bi, Se, Sb, Te, Pb and Cu (Goldfarb et al., 2005; Reis et al., 2004). Maps of factor analysis will be produced as well as single element maps for elements that are included in the gold mineralization. Along with single element maps and factor analysis maps, structural observations as well as alteration intensities will be compared with the factor analysis results. The elements grouped in the gold mineralization may also provide additional information about the deposit type.

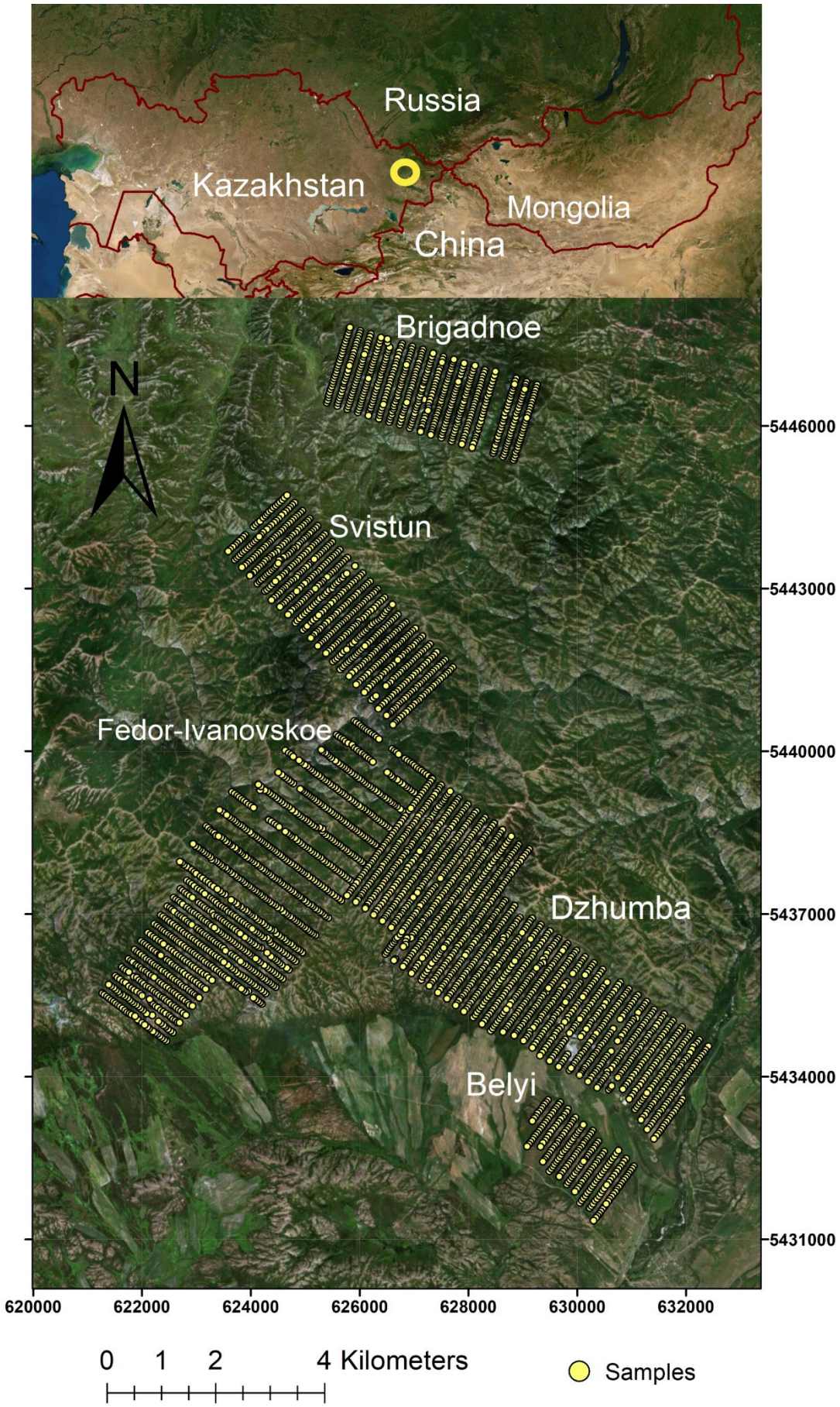

Figure 1. The location of the collected samples as yellow dots, eastern Kazakhstan.

2. GEOLOGICAL SETTING

2.1. Geology of eastern Kazakhstan

Dzhumba gold prospect is located in the Paleozoic sedimentary basin of Irtish-Zaisan terrane which is dominated by accretionary and collisional belts. One of these belts is the western Kalba gold-bearing thrust and fold belt. Dzhumba is situated in the southeastern flank of the western Kalba belt. The western Kalba belt is about 800 kilometers long with a northwest – southeast strike (Kovalev et al., 2009). The western Kalba belt is in contact with two other belts, to the northeast there is the rare earth element rich Kalba-Narym belt and in the southwest there is the Zharma-Saur belt that is dominated by copper, gold and rare metals (Kovalev et al., 2009). Beyond the two surrounding belts, there are the Gorny Altai Caledonides in the northeast and Chingiz-Tarbagatay Caledonides in the southwest (Kovalev et al., 2014). The western Kalba belt extends eastward to China although some authors have classified the portion of the belt east of lake Zaisan as Charsko-Zimunaiskaya (Dyachkov et al., 2018). The western Kalba belt is positioned between two island arcs and it is a terrigenous accretionary complex (Kovalev et al., 2009). Figure 2. shows the lithology surrounding the western Kalba belt as well as the location of Dzhumba, situated in a char suture-shear zone (western Kalba belt).

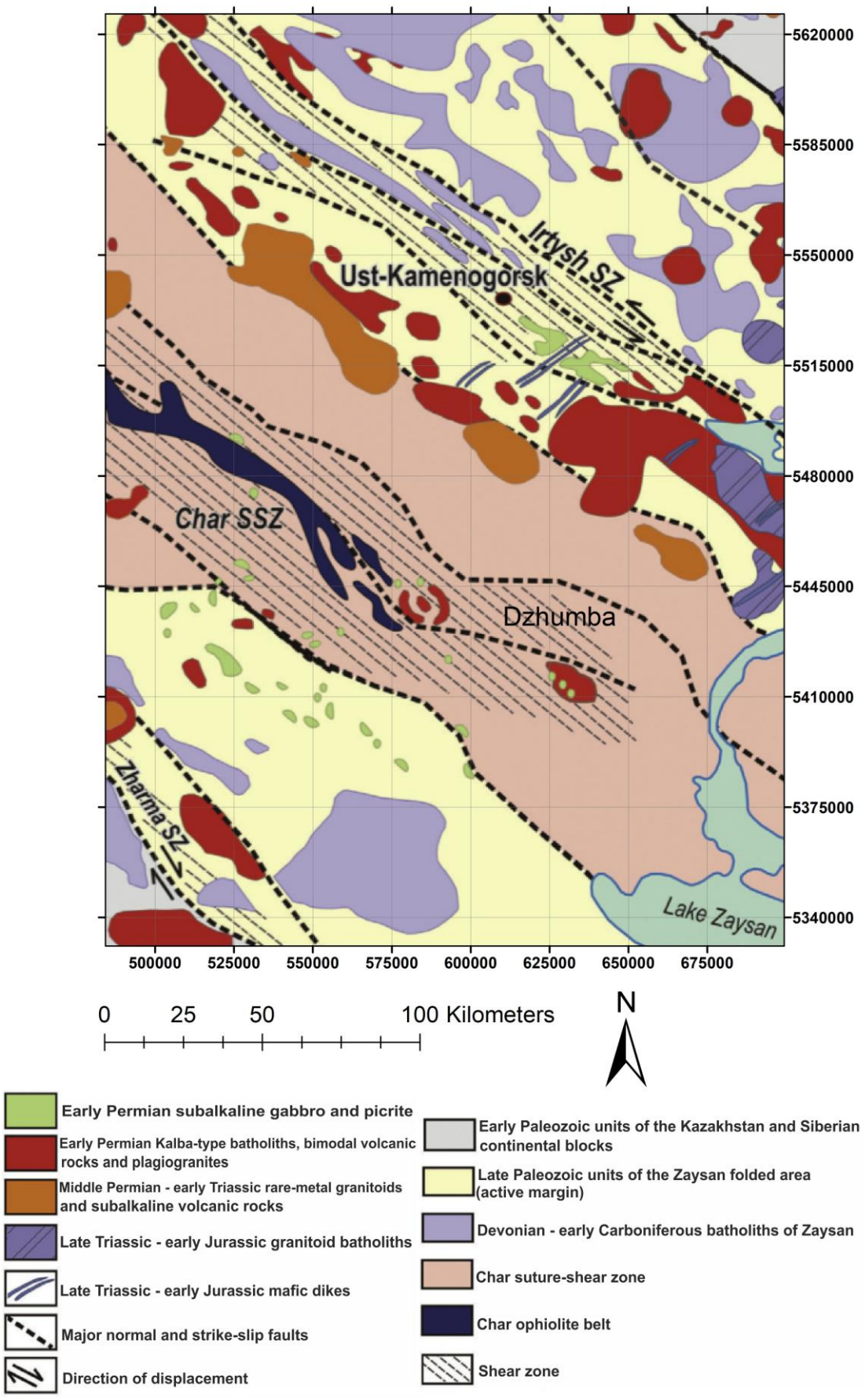

Figure 2. Lithology of western Kalba belt including the location of Dzhumba, modified after Safonova 2014.

The dominant structural component in the western Kalba belt is the Sentash–Kurchum island-arc uplift neighboring the Terekta fault (Kuz'mina et al., 2013). Beneath the uplift, at a depth of 1 to 2 kilometers, there are intrusions of normal to acidic composition (Kuz'mina et al., 2013). Dzhumba is one of the ore clusters on the surface above the intrusions (Kuz'mina et al., 2013). Gold deposits formed in the Zaisan suture zone in a geodynamic setting during the time of collision and are situated within the western Kalba belt and the Irtysh shear zone (Mizernaya et al., 2017).

Gold in the western Kalba belt is usually hosted by sulfides found in black shales and quartz veins found in granitic rocks (Kovalev et al., 2009). The granitoids themselves are found to exhibit high concentrations of Nb, Sn, Be and Li compared to the average crust values (Safonova, 2014). Gold deposits in black shales are promising exploration targets as they host great volumes of ore (Bespayev et al., 2018). Black shales are broadly spread in the geotectonic structures of the western Kalba belt. This is specifically due to molasse which functioned as a geochemical foundation for metamorphic processes that led into the formation of gold-carbon-sulphide deposits (Bespayev et al., 2018).

Also, gold-quartzite/quartz veins are abundant, and they are hosted by low-carbon greywacke sediments. The emplacement of gold-bearing quartzite/quartz veins was fault controlled and genetically linked with small intrusions and dikes belonging to Kunush/Kunushsky complex. This complex is dated to be 309 – 299 Ma old (Kovalev et al., 2014). All the vein-hosted deposits in the area are also associated by gold placer deposits (Bespayev et al., 2018; Mizernaya et al., 2017).

2.2. Dzhumba and other gold deposits of the study area

Dzhumba is the largest of the known gold deposits in the study area. It is hosted by clastic sedimentary including tuffaceous sandstone with graphitic shales with volcano-sedimentary sequences. The gold deposit type for Dzhumba is interpreted to be the Kulujun type, which represents gold-quartzite/quartz veins among terrigeneous, carbonaceous rocks (Bespayev et al., 2018). The gold itself can be native/visible gold or invisible gold. Visible gold is only found in the quartz veins (Bespayev et al., 2018).

Invisible gold is very finely scattered into sulfides, namely pyrite and arsenopyrite and as well into carbonaceous matter (Bespayev et al., 2018).

Dzhumba also displays antimony mineralization along the gold-quartz and gold-sulfide veins. Antimony is believed to have deposited during the paragenesis of gold-sulfide mineralization at relatively high temperatures of 250 – 310 °C (Kovalev et al., 2014).

Gold mineralization is structurally controlled and its associated alteration styles can be categorized into proximal, intermediate and distal zones. The core is quartz veins and/or hydrothermal graphite, proximal zone is ankerite-rich with or without abundant calcite, intermediate zone is ankerite-poor zone with various amounts of calcite and finally distal zone is a calcite zone with no ankerite. The Calcite dissemination steadily declines outwards, and within the most remote parts of distal alteration calcite only occurs in fractures (Peltonen, 2018).

The mineralization type in Dzhumba shows characteristics of an orogenic gold type. This is supported by the presence of hydrothermal quartz veins, alteration related to orogenic gold and occurrence of elements associated with orogenic gold. Well documented processes why gold precipitates from a hydrothermal fluid and forms mineralizations include: 1) The loss of S from the hydrothermal fluid due to sulphidation caused by the surrounding wall rock, 2) by chemisorption, 3) by an oxidation or reduction reaction of the hydrothermal fluid, 4) by immiscibility of H_2S in the fluid, 5) any combination of the listed processes (McCuaig and Kerrich, 1998). Because black shales are present, the hydrothermal fluids may react with graphite in the surrounding wall-rock and produce methane. Graphite acts as a chemical reductant for $Au(HS)_2^-$ fluid (Ridley, 2013). This leads to the precipitation of gold as the H_2S in the fluid experiences a reduction reaction (Naden and Shepherd, 1989).

In addition to Dzhumba, several smaller gold prospects are known from the study area: Belyi, Fedor-Ivanovskoe, Svistun, and Brigadnoe. Fedor-Ivanovskoe is a system of 7 parallel quartz-gold-sulfide veins. The veins are hosted in altered narrow shear zones in

shale and sandstone. Belyi is dominated by intensive silicification located in altered shale interbeds hosted in tuffaceous sandstone. In Brigadnoe the main rock type is fine to middle-grained grey sandstone with rare siltsone and silt-sandstone layers. There is also a presence of igneous andesite stocks. Svistuin rocks are mostly coarse and fine-grained sandstones and siltstones, but there is also a presence of mafic volcanic rocks and quartzite bodies as well as milky quartz veins (Peltonen, 2017, 2018). In order to avoid confusion with the names, Dzhumba project area is used when discussing about all of the gold prospects combined.

3. FACTOR ANALYSIS

Factor analysis is a statistical method of taking enormous amounts of data and then shrinking it to a reduced data set that is easier to comprehend. It is a tool for discovering patterns that might be hidden, show the overlapping of those patterns and express the features that can be found in the hidden patterns (Mäkinen, 1989). Factor analysis produces factors from variables (e.g. from element compositions) that have comparable response patterns in relation to each other (Marsh et al., 1998). The variables are linked through an unseen variable that isn't directly measured and doesn't exist in the data set (Healy, 2013). For example, if nickel, copper, platinum and palladium responded the same way and therefore were put together in a factor, they would be linked and associated by an unmeasured variable, a Ni-Cu-PGE deposit variable. In factor analysis, there are as many factors as the total number of variables in the data set. A single factor explains some sum of the total variance and the factors are numbered according to the amount of variation they describe from highest to lowest.

The amount of how much variance a factor captures is called an eigenvalue. Eigenvalue of 1 means that the factor explains the same amount of variance as a single variable. In factor analysis it is desirable that the factor explains as much of the variance as possible, so eigenvalues above 1 are generally used and the factors with eigenvalue below 1 are usually discarded. The connection of a variable to a factor is called factor loading. Factor loadings range from 1 to -1. If the factor loading is 0, it has no effect on the variable and the closer it is to either limit, 1 or -1, the more impact it has on the variable.

The ideal scenario would be, that the factor analysis will return a small number of factors. The factors then should have elevated factor loadings (more than 0.5) for linking and correlating variables and poor factor loadings for other variables that do not possess correlating response patterns (Healy, 2013). This would make the detection of hidden variables much easier.

Factor analysis also produces factor scores. Factor scores are values indicating how much the resulting factor has been influenced by the variable (e.g. element) of an observation (e.g. soil sample). Factors themselves are in essence geochemical associations that have been obtained from the geochemical data set. Defining how strongly a geochemical association (the factor) is expressed in the elemental composition of the samples is done using factor scores. SPSS program generates factor scores for all the resulting factors and for every single soil sample data point. Factor scores can be used as new variables with a numerical value and a coordinate (of the soil sample). This allows the mapping of geochemical associations (factors) in GIS programs (Healy, 2013).

Before factor analysis can be performed, the data should be log-transformed. This is because the element concentrations in geochemical data commonly varies greatly. There are major-, minor- and trace-elements with hugely different concentrations from tens of percentages to as low as parts per million. This is a slight problem, because a big numerical variance will have the highest effect on the outcome. This means major elements with huge absolute numerical extents will dwarf the importance of minor elements and especially trace elements (Reimann et al., 2002). Solution for this issue is log-transformation. The usefulness of log-transformation can be seen when comparing the ranges of Mg and Au, and the log-transformed ranges of Mg and Au in the data set. The raw data of Mg has a range of 25111 and Au has a range of 0.881. When log-transformed, Mg now has a range of 0.89 and Au has a range of 2.64. This underlines the elements that have large variation and makes the elements equal in terms of absolute range. The minor and trace elements do not get overrun by huge amounts of major elements (Reimann et al., 2002). If the data was on different metrics, e.g. some elements presented as ppm and others as ppb, a standardization to zero mean should be carried out

(DiStefano et al., 2009). Fortunately, all of the data is in ppm, so no standardization is needed.

There are two types of factor analysis: confirmatory and exploratory factor analysis (Osborne, 2014). Confirmatory is used when there is a clear understanding of the problem and as the name conveys, it is used to confirm a hypothesis. Exploratory factor analysis is used when not much is known about the problem and the program is given flexibility in some parameters to complete the analysis. In this thesis exploratory factor analysis will be used.

There are also two exploratory factor analysis methods that can be used, maximum likelihood and principal axis factoring. Principal axis factoring hypotheses less statistical assumptions than maximum likelihood and it works better for data that is not normally distributed (Osborne et al., 2008; Reimann et al., 2002). There is another analysis method named principal component analysis, which is a common analysis method that is associated with exploratory factor analysis. However it is not a true factor analysis and it is often confused as a method of exploratory factor analysis (Reimann et al., 2002). Their major difference is that principal component analysis will show the complete structure of the data and force all variables into the result. It has the intent of explaining the same amount of variance with fewer variables (Reimann et al., 2002; Suhr, 2005). Exploratory factor analysis on the other hand is relying on the correlation structure of the variables and it allows for some factors to have totally different demeanor than the rest (Reimann et al., 2002). This basically means that underlying common structures are more easily detected, giving factor analysis an edge over principal component analysis regarding geochemical data set analysis (Reimann et al., 2002; Suhr, 2005).

Because of the nature of factor analysis excluding unique variance and factor generation happens only from common variance, its spatial accuracy and definition detail is expected to be much greater than what a corresponding univariate (e.g. a single element spatial distribution map) data would be (Healy, 2013).

Rotations are an important part in factor analyses. Rotations can be oblique or orthogonal. Oblique rotations create factors that are correlated with each other whereas orthogonal rotations do not presume that factors are correlated (Reimann et al., 2002). Rotations make the factors to be easier to understand and help with interpretations.

4. MATERIALS AND METHODS

4.1. Samples

The studied samples represent surficial regolith. Samples (0.5-1 kg) were collected by the Aurora Exploration Oy (ltd) field-team using shovel from 0.2-0.5 meter deep pits, sieved in-site using 2 mm sieve. Fine fraction was packed into plastic bags and sent to ALS laboratory at Kyrgyzstan. Points along a soil sample lines were 50 meters apart, and distance between two parallel soil sample lines was 200 meters. Figure 1. shows the locations of the sample points on a map.

At ALS laboratory samples were assayed using four acid total digestion and ICP-MS finish. Some elements, such as Ge, Hg and Re had concentrations under their detection limits. Also, the elements Al and Ti were above their detection limits. These elements cannot be used in factor analysis and therefore have to excluded from the data set. Data for Ag, Te and Se is mostly under the detection limit, but not entirely. They will be included in the analysis, but this has to be kept in mind when interpreting the results.

4.2. Analysis methods

The computer program used to perform factor analysis for this thesis is IBM's SPSS software. The GIS software for producing maps is ESRI's ArcGIS. The elements have been log-transformed in SPSS.

Exploratory factor analysis will be used instead of principal component analysis. In order to decide which exploratory analysis method should be used, the data should be tested

whether it is normally distributed or not. A Shapiro-Wilk test reveals that neither our raw data nor log transformed data is normally distributed (Table 7. found in the appendix section). They all have values of 0.000 whereas a value of 0.05 or above would indicate that the data is normally distributed (Shapiro and Wilk, 1965). Hence, principal axis factoring will be used as the primary factor analysis method as it works best for non-normal data (Osborne et al. 2008). When considering rotations, Reimann et al. (2000) suggests that varimax works the best for principal axis factoring analysis as the rotation method. Hence, varimax orthogonal rotation with Kaiser normalization will be used in these analyses.

At first, the number of factors will not be fixed to a certain number. The only limitation is that the eigenvalues of the factors have to be above or exactly 1. The scree plot and its slope that is produced will however give an indication of how many factors are essential, and a new factor analysis with a fixed number of factors can be performed. Usually in scree plots there will be an "elbow" in the curve, and the number of factors above the elbow are commonly regarded as essential. However in exploratory factor analysis it is not uncommon to try including one or two factors from below the elbow as well (Osborne et al., 2008). In a confirmatory factor analysis, factor loadings below 0.7 could be excluded or left blank due to the nature of the analysis. But because this is an exploratory factor analysis, factor loadings less than 0.25 are excluded. This is done in order to make the factors simpler and clearer to understand and at the same time by choosing a low value of 0.25, giving enough room for lesser factor loadings to present themselves.

5. RESULTS

5.1. Statistical analysis

Representative original chemical analysis used in this study is found in Table 8. in the appendix section. Table 1. below consists of general descriptive statistics of the data. Table 1. reveals that skewness is positive for most of the elements. Range shows that the absolute values for different elements differ considerably. Hence a log transformation is necessary to perform.

Table 1. The descriptive statistics for the data set.

	Range	Minimum	Maximum	Sum	Mean	Std. Deviation	Skewness
Au	0.881	0.002	0.883	41.562	0.01054	0.04	12.168
Ag	3.0	1.0	4.0	3965.2	1.006	0.09	22.112
As	2256.0	3.0	2259.0	123431.0	31.312	53.22	21.503
Ba	3054.0	170.0	3224.0	1836709.0	465.933	79.05	14.063
Be	3.9	0.5	4.4	8077.2	2.049	0.36	1.681
Bi	1.62	0.03	1.65	1284.03	0.3257	0.06	5.335
Ca	47622.0	2378.0	50000.0	46735585.0	11855.805	4524.93	4.533
Cd	2.7	0.2	2.9	1772.6	0.450	0.16	5.104
Ce	128.0	7.0	135.0	255718.5	64.870	10.86	0.333
Co	88.0	4.6	92.6	107543.1	27.281	9.03	1.652
Cr	377.0	38.0	415.0	273305.0	69.332	12.12	13.921
Cu	367.0	16.0	383.0	165607.0	42.011	18.98	5.541
Fe	28091.0	21909.0	50000.0	159827876.0	40544.870	4236.25	-0.062
Ga	44.4	2.6	47.0	77946.2	19.773	2.05	0.571
K	36062.0	7322.0	43384.0	78302670.0	19863.691	2148.47	-0.014
La	69.6	2.5	72.1	110492.0	28.029	4.23	0.647
Li	82.0	17.0	99.0	142484.0	36.145	5.01	2.045
Mg	25111.0	3708.0	28819.0	43226534.0	10965.635	1578.14	0.486
Mn	9702.0	298.0	10000.0	5763274.0	1462.018	701.56	5.339
Mo	13.2	0.2	13.4	5849.9	1.484	0.59	8.887
Na	22996.0	2223.0	25219.0	45567268.0	11559.429	1783.30	0.540
Nb	23.3	1.1	24.5	38026.7	9.647	1.42	0.031
Ni	468.0	24.0	492.0	159443.0	40.447	12.39	22.679
P	2350.0	605.0	2955.0	5195554.0	1317.999	277.23	0.937
Pb	212.0	3.0	215.0	100332.5	25.452	10.66	3.650
Rb	226.0	8.0	234.0	372529.0	94.503	14.40	-0.235
S	3186.0	179.0	3365.0	3282402.0	832.674	282.90	1.626
Sb	43.2	0.2	43.4	6876.4	1.744	1.47	11.546
Sc	30.0	8.0	38.0	58636.0	14.875	1.86	1.833
Se	7.5	1.5	9.0	7898.0	2.004	0.84	2.670
Sn	20.4	0.2	20.6	8419.7	2.136	0.54	12.895
Sr	481.0	61.0	542.0	709810.0	180.063	36.95	1.714

Table 1. continued

	Range	Minimum	Maximum	Sum	Mean	Std. Deviation	Skewness
Ta	1.97	0.08	2.05	2710.84	0.6877	0.11	0.466
Te	6.0	5.0	11.0	19842.8	5.034	0.25	10.158
Th	27.9	1.0	28.9	37230.1	9.444	1.51	0.392
Tl	1.4	0.1	1.5	1834.7	0.465	0.08	1.151
U	10.4	0.3	10.7	10417.5	2.643	0.60	3.230
V	149.0	49.0	198.0	409719.0	103.937	12.68	0.531
W	30.0	1.0	31.0	7060.0	1.791	0.71	18.138
Y	63.9	2.2	66.1	80620.9	20.452	2.90	2.658
Zn	332.0	42.0	374.0	399922.0	101.452	19.45	3.412
Zr	159.0	41.0	200.0	311326.0	78.977	10.91	2.293

Table 2. is the descriptive statistics with log transformed data. It shows that the skewness has been reduced considerably compared to the raw data. Also the range between the elements is now in the same magnitude.

Table 2. The descriptive statistics for the log transformed data.

	Range	Minimum	Maximum	Sum	Mean	Std. Deviation	Skewness
logAu	2.64	-2.70	-0.05	-9441.97	-2.3952	0.43232	1.935
LogAg	0.60	0.00	0.60	6.72	0.0017	0.2277	17.695
logAs	2.88	0.48	3.35	5425.90	1.3764	0.25517	1.947
logBa	1.28	2.23	3.51	10502.20	2.6642	0.05771	0.865
logBe	0.94	-0.30	0.64	1204.42	0.3055	0.07091	0.562
logBi	1.74	-1.52	0.22	-1950.51	-0.4948	0.08054	-0.183
logCa	1.32	3.38	4.70	15980.39	4.0539	0.12287	1.179
logCd	1.16	-0.70	0.46	-1447.18	-0.3671	0.12519	0.802
logCe	1.29	0.85	2.13	7118.42	1.8058	0.07504	-0.827
logCo	1.30	0.66	1.97	5579.19	1.4153	0.13078	0.382
logCr	1.04	1.58	2.62	7241.84	1.8371	0.05331	2.719
logCu	1.38	1.20	2.58	6296.92	1.5974	0.13781	1.361
logFe	0.36	4.34	4.70	18154.93	4.6055	0.04622	-0.427
logGa	1.26	0.41	1.67	5099.61	1.2937	0.04690	-1.910
logK	0.77	3.86	4.64	16932.43	4.2954	0.04905	-1.131
logLa	1.46	0.40	1.86	5686.51	1.4425	0.06780	-1.255
logLi	0.77	1.23	2.00	6126.81	1.5542	0.05682	0.403
logMg	0.89	3.57	4.46	15907.32	4.0353	0.06521	-1.016
logMn	1.53	2.47	4.00	12365.16	3.1368	0.14351	1.179
logMo	1.83	-0.70	1.13	606.86	0.1539	0.11119	1.730
logNa	1.05	3.35	4.40	15995.40	4.0577	0.06854	-0.742
logNb	1.34	0.05	1.39	3860.00	0.9792	0.06948	-1.667

Table 2. continued

	Range	Minimum	Maximum	Sum	Mean	Std. Deviation	Skewness
logNi	1.31	1.38	2.69	6305.60	1.5996	0.06885	3.792
logP	0.69	2.78	3.47	12262.69	3.1108	0.08859	0.142
logPb	1.86	0.48	2.33	5414.66	1.3736	0.16758	-0.157
logRb	1.47	0.90	2.37	7765.15	1.9698	0.07258	-1.820
logS	1.27	2.25	3.53	11426.12	2.8986	0.13561	0.307
logSb	2.34	-0.70	1.64	757.72	0.1922	0.17279	2.178
logSc	0.68	0.90	1.58	4609.38	1.1693	0.05161	0.548
logSe	0.78	0.18	0.95	1086.91	0.2757	0.13772	1.662
logSn	2.01	-0.70	1.31	1263.17	0.3204	0.08726	-0.183
logSr	0.95	1.79	2.73	8858.94	2.2473	0.08223	0.554
logTa	1.41	-1.10	0.31	-665.62	-0.1689	0.07606	-1.393
logTe	0.34	0.70	1.04	2765.10	0.7014	0.01832	8.795
logTh	1.45	0.01	1.46	3820.32	0.9691	0.07500	-1.489
logTl	1.18	-1.00	0.18	-1337.69	-0.3393	0.08017	-0.625
logU	1.55	-0.52	1.03	1625.77	0.4124	0.09011	0.072
logV	0.61	1.69	2.30	7937.39	2.0135	0.05312	-0.240
logW	1.49	0.00	1.49	909.30	0.2307	0.14108	-0.488
logY	1.48	0.34	1.82	5151.04	1.3067	0.05931	-0.738
logZn	0.95	1.62	2.57	7883.41	1.9999	0.07178	1.201
logZr	0.69	1.61	2.30	7465.47	1.8938	0.05520	0.929

5.2. Factor analysis results

First factor analysis is tested with no preset of factors, though only 10 most significant factors are being presented in Table 3. in order to clarify the results and reduce confusion from unnecessary factors.

Table 3. Rotated factor matrix. Total variance explained by ten factors is 72.822%. Extraction method: Principal Axis Factoring. Rotation method: Varimax with Kaiser normalization.

Factor	1	2	3	4	5	6	7	8	9	10
Nb	0.926									
Th	0.901									
Ta	0.878									
Rb	0.846	-0.276								
Tl	0.808									
Bi	0.785		0.340							
La	0.726					0.398		0.286		
Sn	0.697									
Ce	0.674									

Table 3. continued

	1	2	3	4	5	6	7	8	9	10
U	0.552		0.262							
W	0.550									
K	0.539				0.442					
Be	0.533							0.270		
Ca	-0.487	-0.324			-0.477				0.318	
Zr	0.468			0.407	0.385	0.266				0.313
Fe		0.893								
V		0.865								
Sc		0.734		0.322		0.273				
Ga	0.343	0.710								
Co		0.604	0.455							
Mg		0.565		-0.466						
S	-0.327	-0.560	0.393		-0.405					
Na		0.494	-0.466						0.340	
P			0.712							
Mn			0.690							0.380
Zn			0.686							
Mo			0.633							
Cd			0.613							
Cu			0.609	0.262		0.258				0.260
Se										
As				0.871						
Au				0.792						
Sb			0.313	0.727						
Ba	0.454				0.550					
Y	0.422	0.281				0.611				
Cr	0.277	0.254					0.678			
Ni			0.419			0.363	0.541			
Te										
Pb								0.637		
Sr	-0.412	0.283							0.723	
Li	0.325	0.345								0.442
Ag										

The scree plot is seen in Figure 3. The scree plot displays the slope of the eigenvalues. It is derived from the rotated factor matrix in Table 3. Figure 3. reveals that the first five factors have the most significant impact as they are above the “elbow”. The slope becomes notably less steep after the sixth factor. Thus, the analysis will be performed again using a fixed number of five factors (Table 4.) instead of using no limit to the

number of factors (as long as eigenvalue is above or equal to one). Because the nature of this analysis is exploratory, it is encouraged to experiment with your data (Osborne et al., 2008). Hence, also an analysis with a fixed number of six factors can be performed as well (Table 5.).

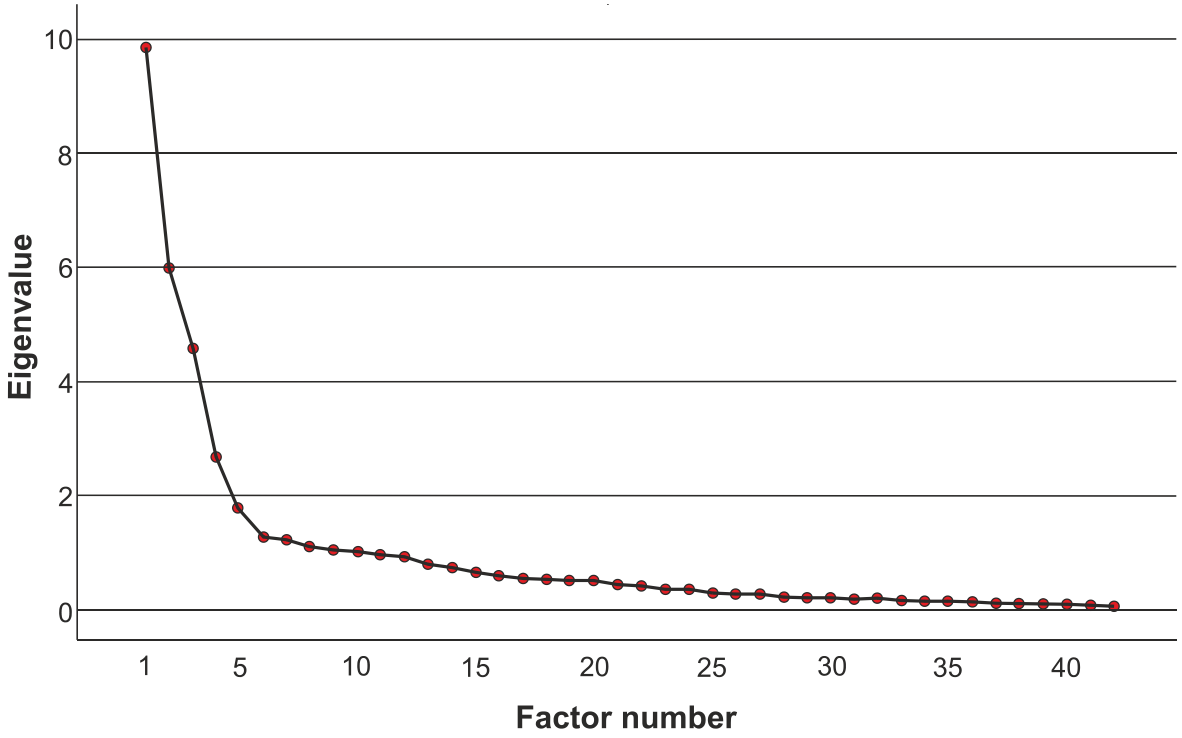

Figure 3. Analysis showing the slope of the eigenvalues.

Table 4. Rotated factor matrix. Preset of 5 factors. Total variance explained by five factors is 59.249%. Extraction method: Principal axis factoring. Rotation method: Varimax with Kaiser normalization.

Factor	1	2	3	4	5
Th	0.918				
Nb	0.891			-0.259	
Ta	0.862			-0.274	
Rb	0.849	-0.298			
Tl	0.828				
La	0.786				
Bi	0.777		0.334		

Table 4. continued

Factor	1	2	3	4	5
Ce	0.717				
Sn	0.676				
K	0.602			0.271	-0.274
Ca	-0.554	-0.265			0.328
Be	0.549				
W	0.526				
U	0.522				
Ba	0.518				-0.332
Sr	-0.467	0.309	-0.309		0.345
Y	0.462	0.302			
Fe		0.918			
V		0.890			
Sc		0.757		0.368	
Ga	0.345	0.676			
Co		0.605	0.395		0.306
Mg		0.540		-0.501	
S	-0.398	-0.531	0.418		
Li	0.336	0.353			
Ag					
P			0.733		
Zn		0.260	0.644		
Mn			0.623	0.345	
Cd			0.619		
Mo			0.569	0.273	
Cu		0.293	0.558	0.364	0.325
Na		0.504	-0.548		

Table 4. continued

Factor	1	2	3	4	5
Ni		0.301	0.410	0.274	
Se					
As				0.792	
Sb				0.782	
Au				0.712	
Zr	0.540			0.543	
Pb					0.455
Cr	0.318	0.320			-0.428
Te					

Table 5. Rotated factor matrix. Preset of 6 factors. Total variance explained by six factors is 62.329%. Extraction method: Principal axis factoring. Rotation method: Varimax with Kaiser normalization.

Factor	1	2	3	4	5	6
Th	0.918					
Nb	0.887			-0.259		
Ta	0.857			-0.265		
Rb	0.848	-0.300				
Tl	0.826					
La	0.788					
Bi	0.782		0.340			
Ce	0.717					
Sn	0.674					
K	0.601					-0.310
Ca	-0.560	-0.306				0.471
Be	0.550					
Zr	0.544			0.517		

Table 5. continued

Factor	1	2	3	4	5	6
W	0.524					
U	0.523					
Ba	0.513					-0.318
Sr	-0.465	0.330	-0.275			0.317
Y	0.459	0.260				
Fe		0.895				
V		0.865				
Sc		0.726		0.372		
Ga	0.347	0.715				
Co		0.612	0.427			
S	-0.393	-0.552	0.429			0.258
Mg		0.499		-0.480		
Li	0.336	0.364				
Ag						
P			0.732			
Mn			0.654	0.312		
Zn		0.253	0.645			
Cd			0.620			
Cu		0.309	0.590	0.356		
Mo			0.589			
Na		0.508	-0.524			
Se						
As				0.803		
Sb			0.272	0.788		
Au				0.719		
Cr	0.292				0.777	
Ni			0.423	0.331	0.474	

Table 5. continued

Factor	1	2	3	4	5	6
Te						
Pb						0.416

Table 4. and Table 5. were analyzed using the principal axis factoring method. In addition to principal axis factoring, maximum likelihood method can also be tested to see if the results are similar. Results for maximum likelihood factor analysis are in Table 6.

Table 6. Rotated factor matrix using maximum likelihood and preset of 6 factors. Total variance explained by six factors is 62.329%. Extraction method: Maximum likelihood. Rotation method: Varimax with Kaiser normalization.

Factor	1	2	3	4	5	6
Th	0.910					
Nb	0.902			-0.254		
Ta	0.875			-0.267		
Rb	0.844	-0.297				
Tl	0.813					
Bi	0.795		0.338			
La	0.759					
Ce	0.715					
Sn	0.685					
K	0.585				-0.368	
Be	0.562					
U	0.532					
W	0.531					
Zr	0.513			0.508	-0.267	
Ba	0.484				-0.374	
Y	0.448	0.276				

Table 6. continued

Factor	1	2	3	4	5	6
Fe		0.906				
V		0.871				
Sc		0.730		0.377		
Ga	0.343	0.709				
Co		0.625	0.409		0.266	
S	-0.361	-0.536	0.440		0.324	
Mg		0.516		-0.491		
Li	0.333	0.364				
P			0.728			
Mn			0.652	0.304		
Zn		0.277	0.635			
Cd			0.616			
Cu		0.308	0.587	0.367		
Mo			0.574	0.261		
Na		0.480	-0.538			
Se						
Sb			0.263	0.792		
As				0.787		
Au				0.715		
Ca	-0.515	-0.303			0.558	
Sr	-0.430	0.321	-0.297		0.438	
Pb					0.377	
Cr	0.279					0.813
Ni			0.427	0.341		0.460
Te						
Ag						

Running the analysis again with the maximum likelihood method in Table 6. does not seem to change the loading values significantly. The factors 5 and 6 in Tables 5. and 6. however seem to flip inversely.

5.3. Maps generated from raw data

Single element maps are presented for Au, Sb, As, Zr, Ni, Mn, Sc, Cu, Mo and K. When using a preset of 5 factors, these are the elements that have factor loadings on the most interesting factor, factor 4. The trend seems to be that anomalies are concentrated into the northernmost parts of the area. Au, Sb and As occurrences seem to be very precisely located with pin pointed red areas and a lot of darker green sections indicating an absence of the element. Their difference to the other elements can be clearly seen as Zr, Ni, Mn, Sc, Cu, Mo and K color the map more yellow all around, indicating a more disseminated presence.

Figure 4. shows that gold has a strong presence in southeast. Northern part of the area, Brigadnoe, has barely any gold. In the middle section of Svistun, there seems to be a northwest to southeast aligned presence of gold, as if it was following a structure. Fedor-Ivanovskoe has a moderate gold presence. Figure 5. shows antimony having biggest concentrations in southeast and in Svistun with elongated presence similar to gold. Brigadnoe has slightly elevated antimony concentrations compared to gold. Figure 6. displays arsenic having high concentration in the southeast, but very low presence anywhere else, just a peak in Svistun. Figure 7. exhibits scandium concentrations being moderately high in southeast and southwest. Relatively same concentration levels continue in the north and all in all scandium seems dispersed more evenly around the area. Figure 8. shows high manganese concentrations in Svistun as a massive spot. Rest of the area is relatively empty, but the dominant yellow color would indicate elevated “background” concentrations throughout Dzhumba project area. Figure 9. displays high molybdenum content in Svistun and Brigandoe. Southeast and southwest have only a couple elevated spots of molybdenum. Figure 10. shows high nickel content in Svistun and in Brigandoe. In Brigandoe, the occurrence seems to follow an elongated path in a west-east direction. Similar to manganese, the rest of the Dzhumba project area is

dominated by elevated background nickel content. In Figure 11. zirconium content is high in southeast Dzhumba, Belyi and Svistun. Brigadnoe has a small occurrence with west-east elongation. The middle of Dzhumba project area, Fedor-Ivanovskoe is relatively void of zirconium. Figure 12. shows very high copper concentrations in Svistun. In Brigadnoe and in the southeast there are slight rises in the copper content. Southwestern tip of the area however exhibits moderate elevations of copper. Fedor-Ivanovskoe is relatively empty. Figure 13. shows that the potassium content is acting quite uniquely compared to the other elements. The potassium content has sharp highs and lows close to each other represented by dark red next to dark green. Due to this it is not evenly disseminated into a constant high background value as for example manganese expresses. The highest potassium occurrences are in Svistun, Dzhumba and Belyi.

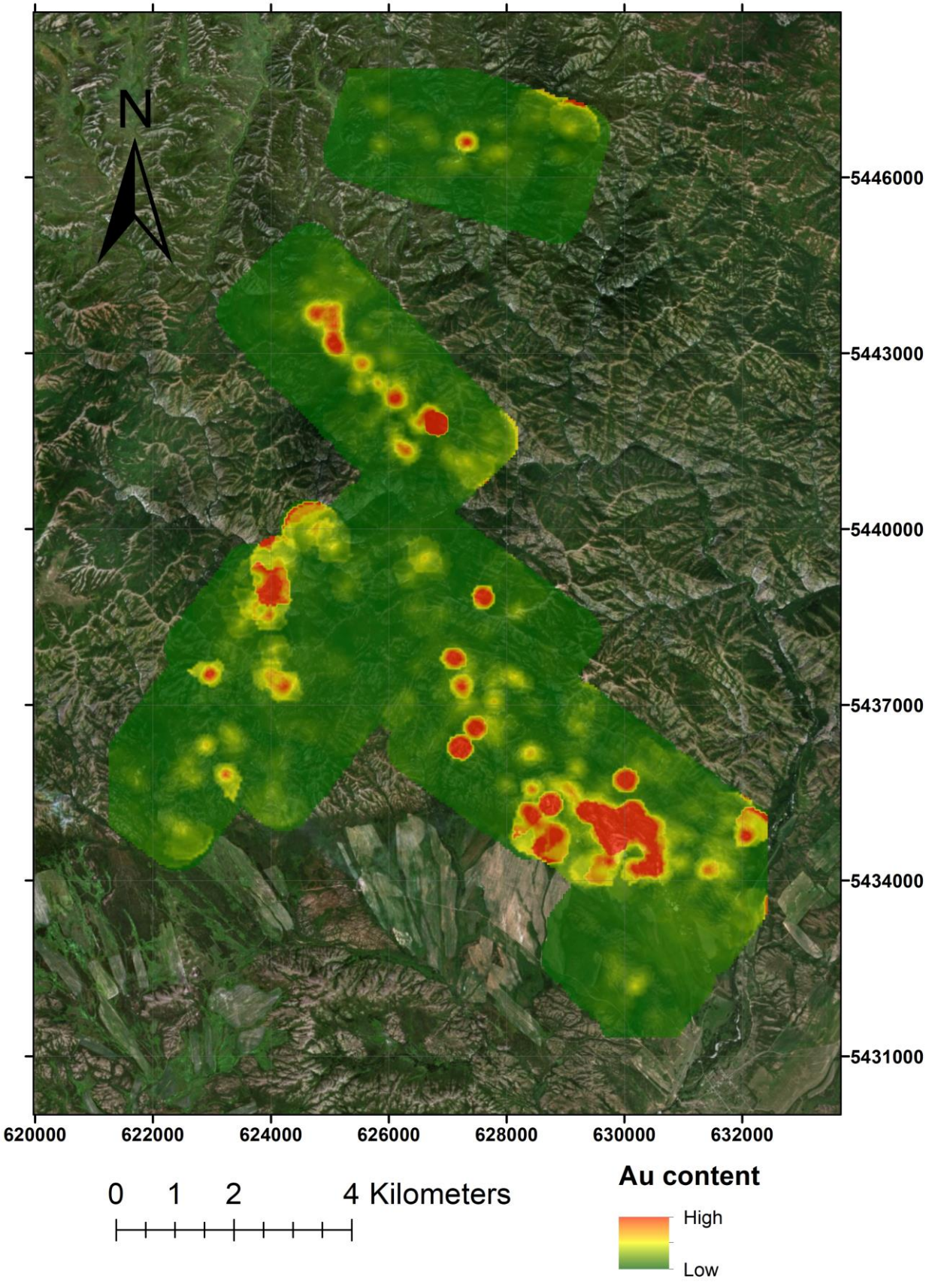

Figure 4. A Kriging interpolation of the gold occurrence produced from the raw data. Area of interpolation is 500 meters from each data point.

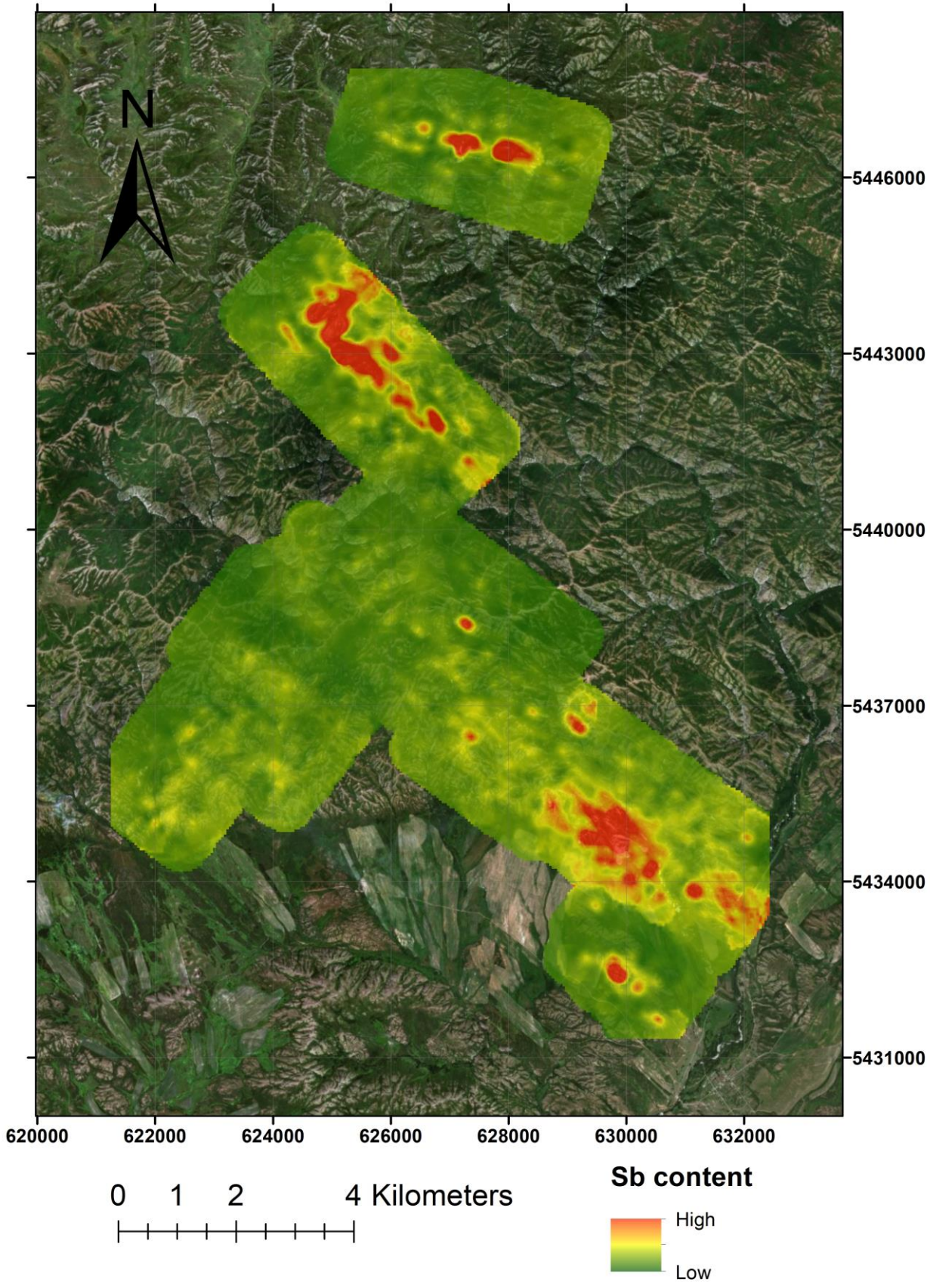

Figure 5. A Kriging interpolation of the antimony occurrence produced from the raw data. Area of interpolation is 500 meters from each data point.

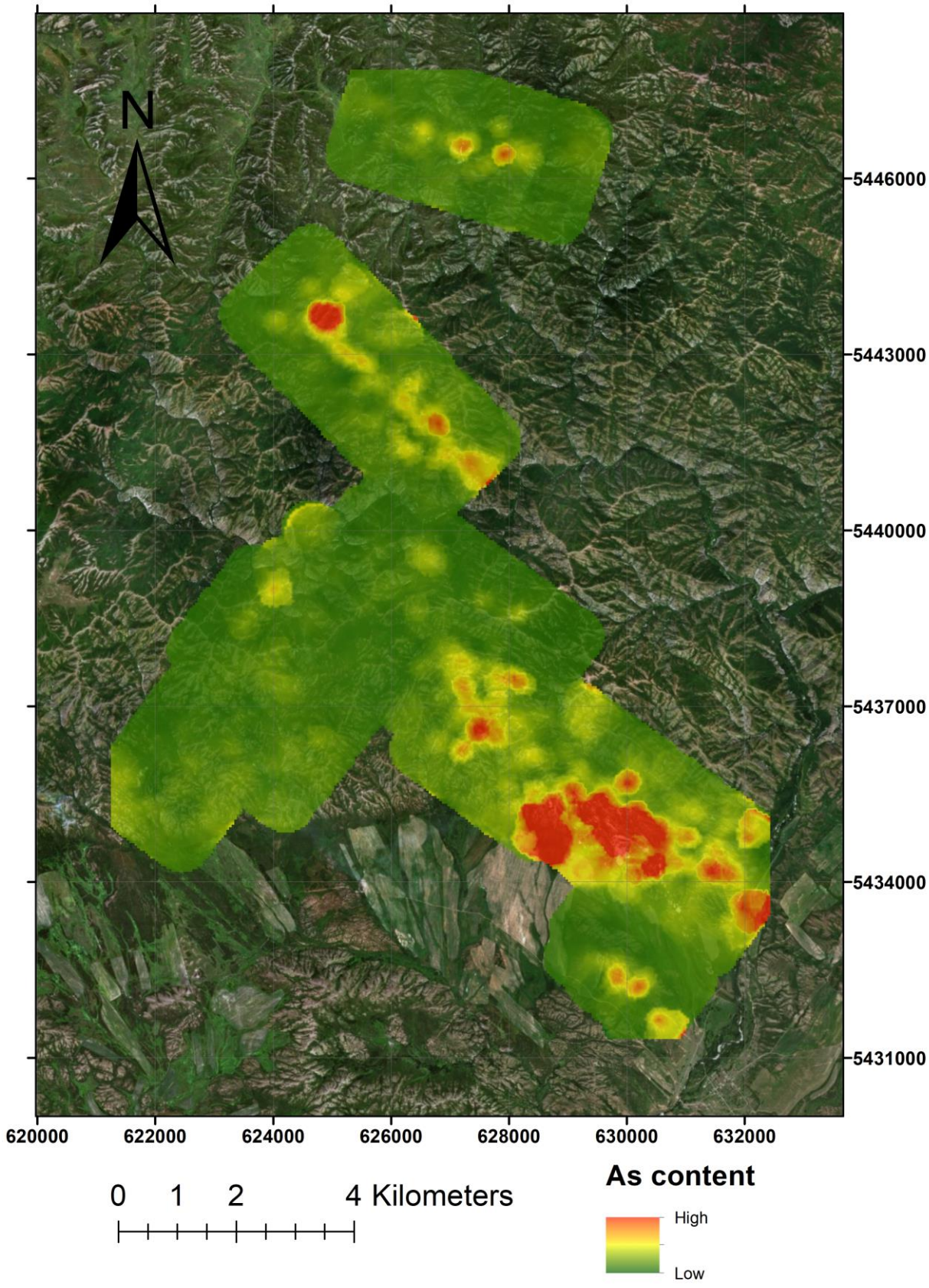

Figure 6. A Kriging interpolation of the arsenic occurrence produced from the raw data. Area of interpolation is 500 meters from each data point.

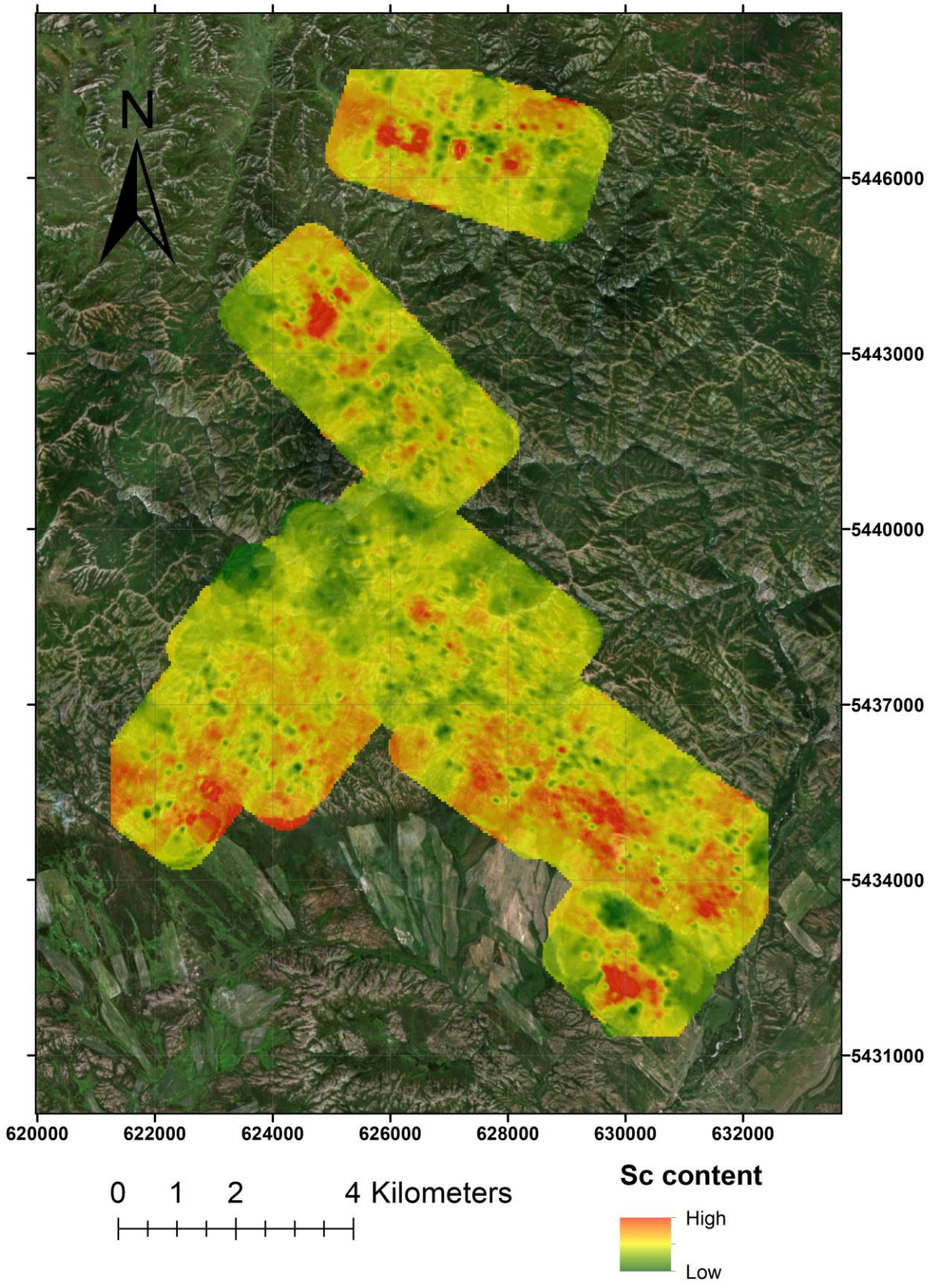

Figure 7. A Kriging interpolation of the scandium occurrence produced from the raw data. Area of interpolation is 500 meters from each data point.

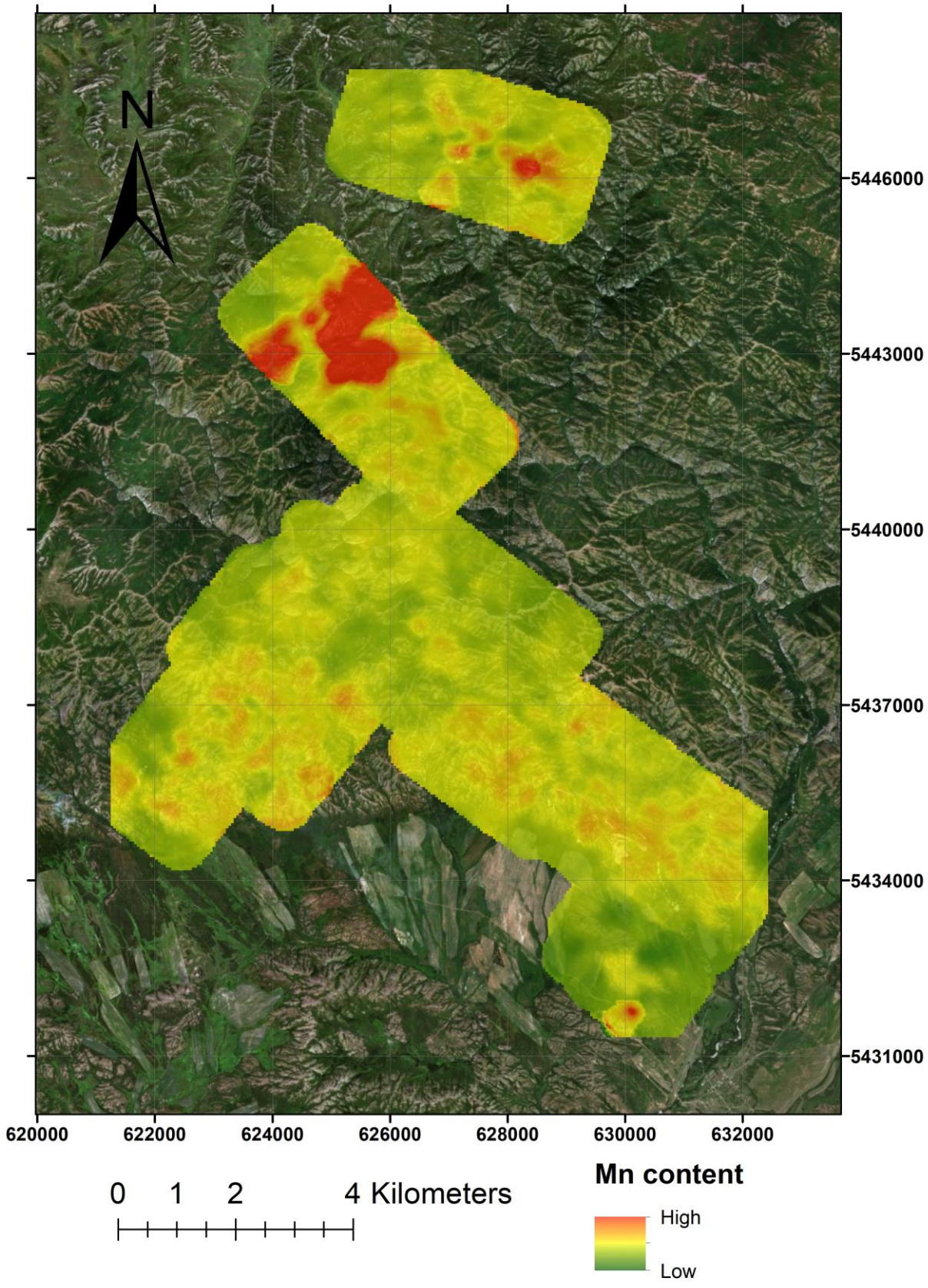

Figure 8. A Kriging interpolation of the manganese occurrence produced from the raw data. Area of interpolation is 500 meters from each data point.

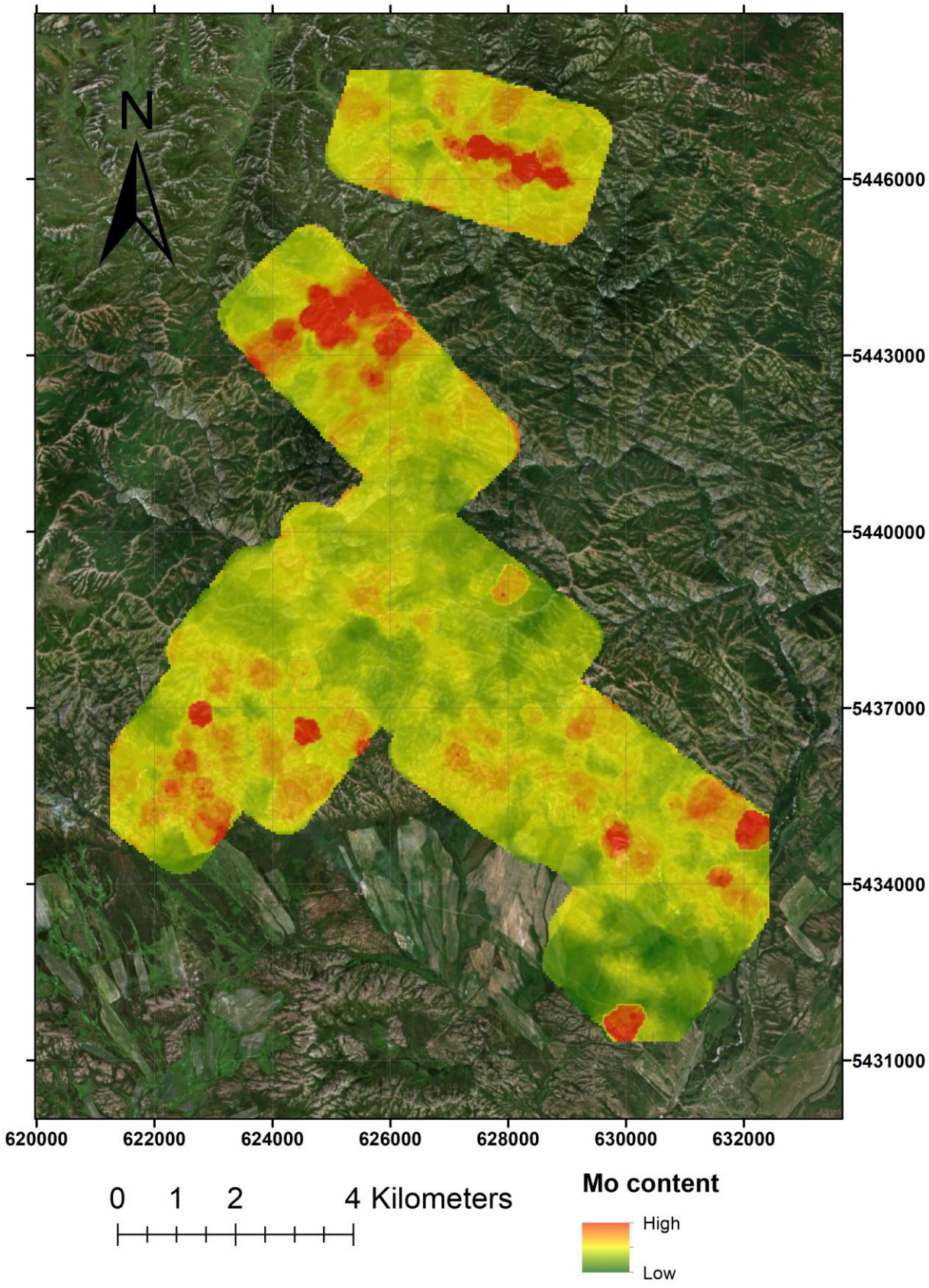

Figure 9. A Kriging interpolation of the molybdenum occurrence produced from the raw data. Area of interpolation is 500 meters from each data point.

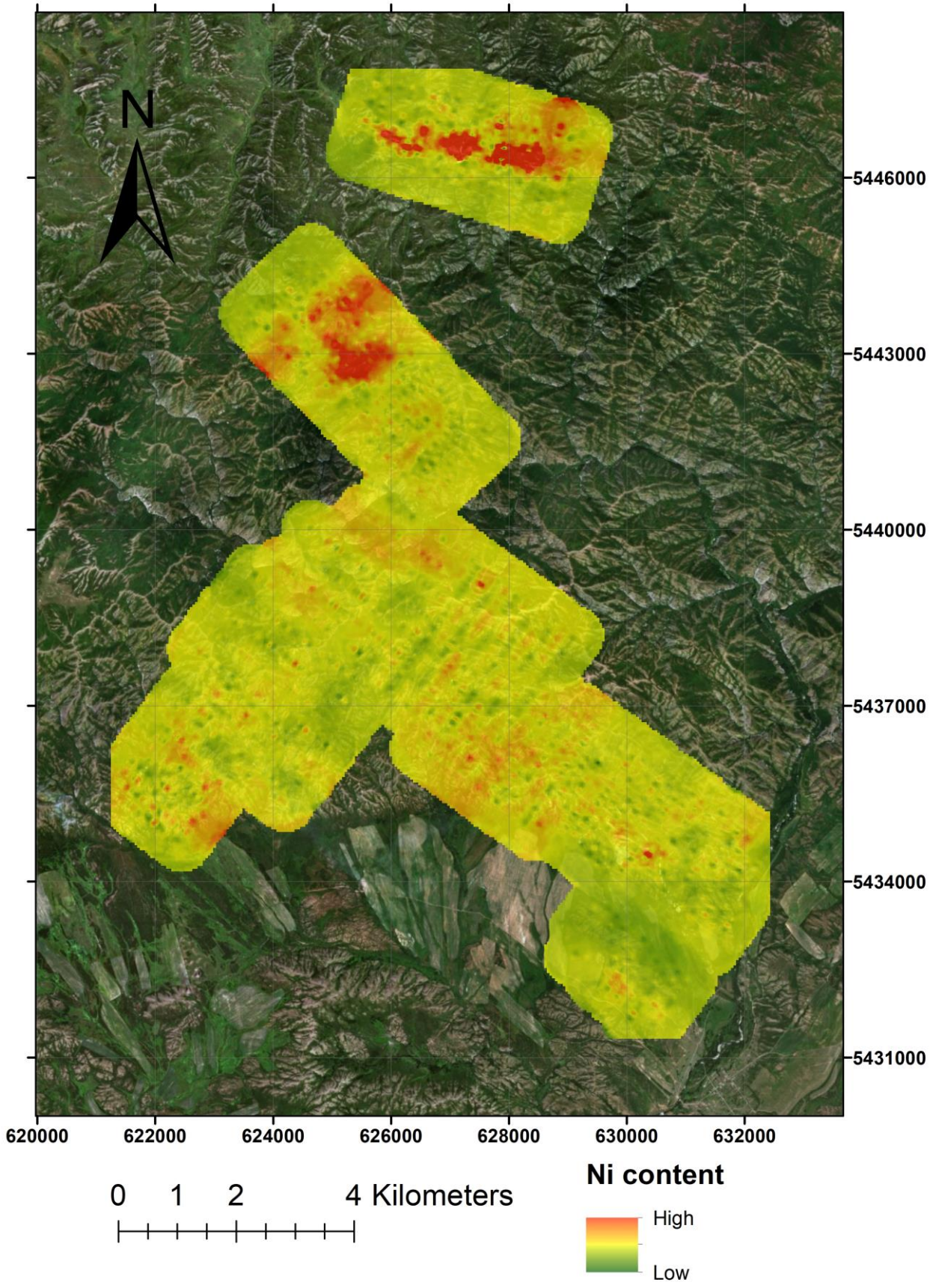

Figure 10. A Kriging interpolation of the nickel occurrence produced from the raw data. Area of interpolation is 500 meters from each data point.

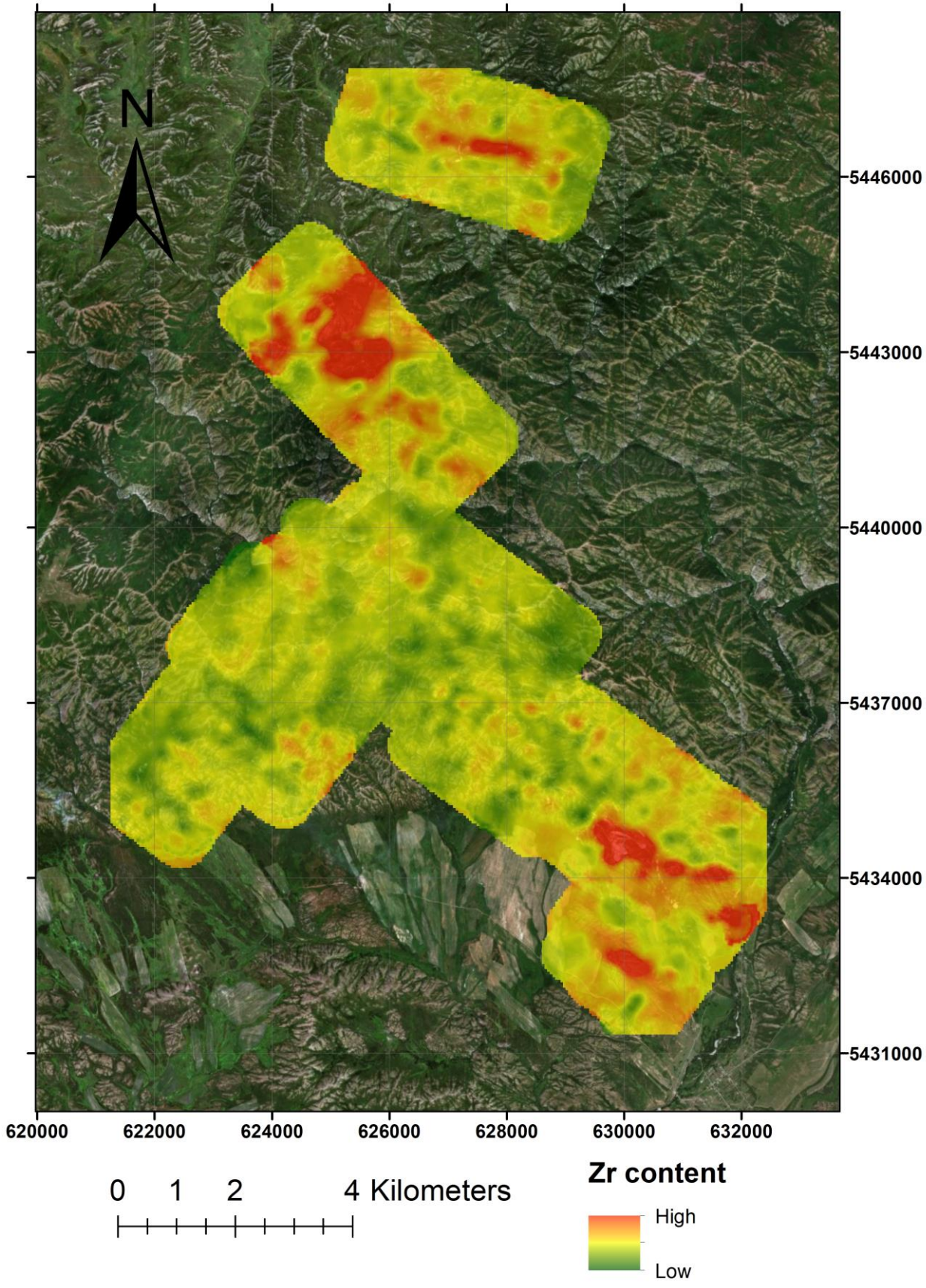

Figure 11. A Kriging interpolation of the zirconium occurrence produced from the raw data. Area of interpolation is 500 meters from each data point.

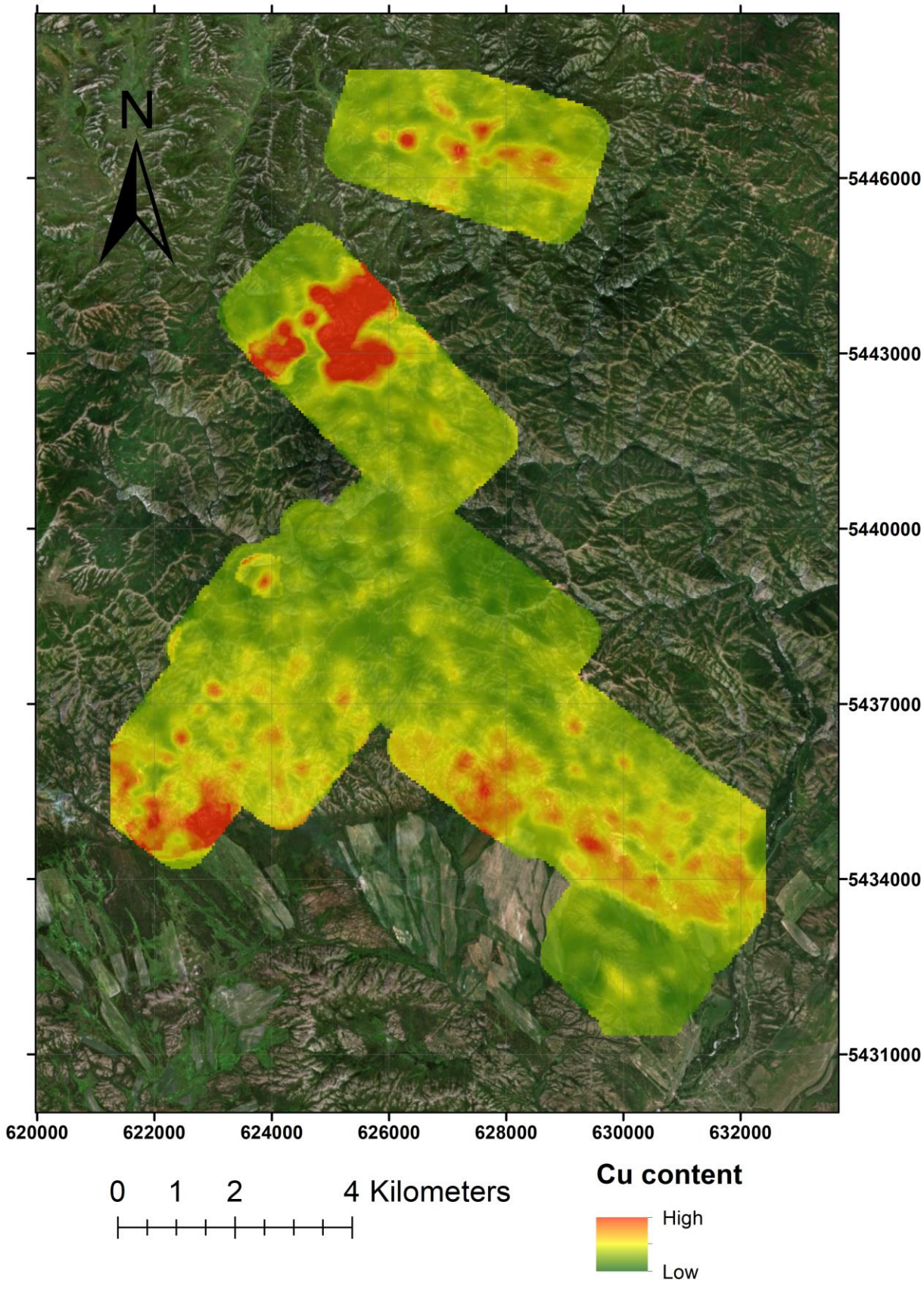

Figure 12. A Kriging interpolation of the copper occurrence produced from the raw data. Area of interpolation is 500 meters from each data point.

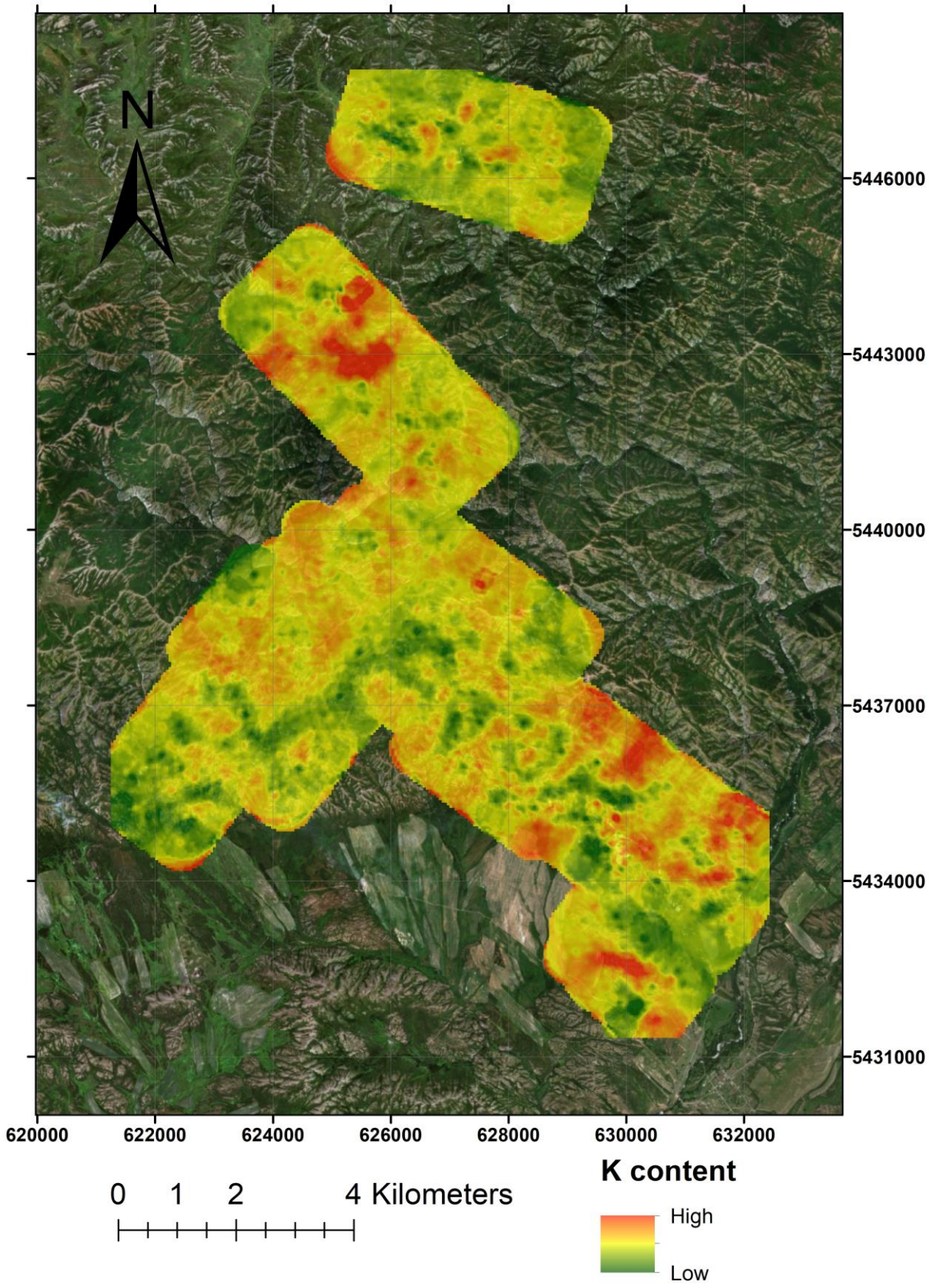

Figure 13. A Kriging interpolation of the potassium occurrence produced from the raw data. Area of interpolation is 500 meters from each data point.

5.4. Maps generated from factor analysis

All five factor maps generated using a preset of five factors are shown below. They are clearly different in relation to each other, meaning the factor scores and their implementation into ArcGIS worked as intended. Also below are the fifth and sixth factor maps with a preset of six factors. Just the fifth and sixth are shown from that set of factors as only they have differences compared to the factor set of five preset factors. The first four maps are not shown as they are practically identical with the first four maps when using a preset of five factors. The final map is the fourth factor generated from the maximum likelihood method results. Only the fourth map is shown just for the sake of presenting it, as all of the maximum likelihood maps are identical to the previous maps. Although the factor loadings and factor scores do vary between different preset of factors used and different analysis methods, the subtle differences do not seem to translate onto maps all that well.

Factor 1 (Figure 14.) has the highest loadings in Svistun and Belyi. Minor to moderate loadings are scattered in the central parts of Dzhumba project area. Factor 2 (Figure 15.) shows high loadings in southwest Fedor-Ivanovskoe and in central parts of Dzhumba project area. Svistun, Belyi and Brigadnoe have small peaks of high loading but they are mostly dominated by low loading intensity. Factor 3 (Figure 16.) displays high loadings for Svistun and Brigadnoe. Fedor-Ivanovskoe has scattered loadings and Belyi has very low loading intensity. Factor 4 (Figure 17.) shows a massive loading for southeast Dzhumba. Svistun and Brigadnoe also have high loadings and they seem to have a west-east or northwest-southeast aligned elongation. Interestingly Fedor-Ivanovskoe seems to be dominated by low loading intensity. Factor 5 (Figure 18.) has high loadings in southeast Dzhumba and the loadings seem to form stripes with a northeast-southwest direction. Fedor-Ivanovskoe has moderately high loadings in the southwest and Svistun and Belyi have small peaks of higher loading although they have lots of low loading intensity as well.

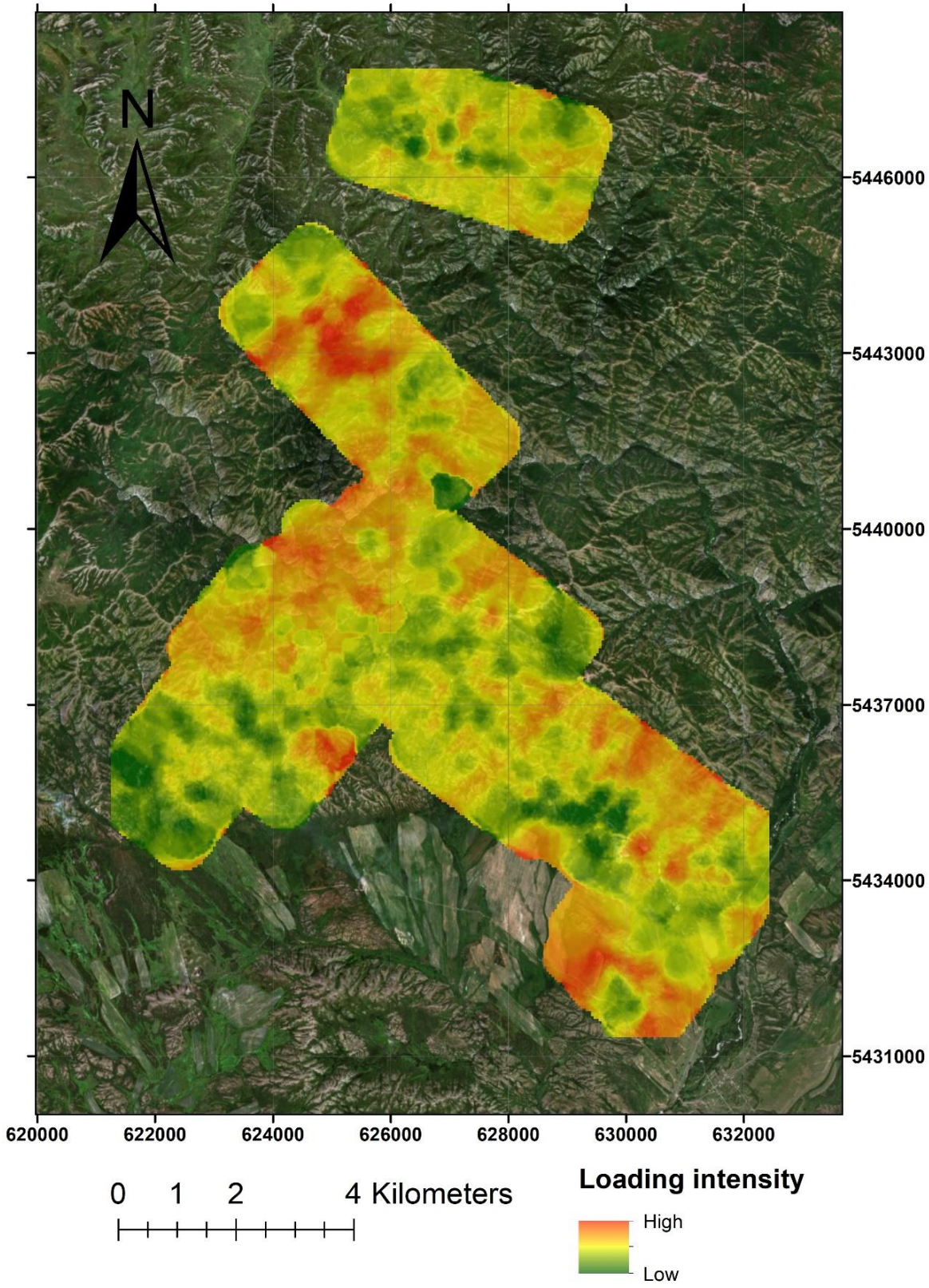

Figure 14. Factor 1. Preset of 5 factors were used. Kriging interpolation of the first factor with 500 meter coverage from data points. Factor 1 explains 23,466% of the total variance and includes positive loadings for Th, Nb, Ta, Rb, Tl, La, Bi, Ce, Sn, K, Be, Zr, W, U, Ba, Y, Ga, Li, and Cr. Negative loadings for Ca, Sr and S.

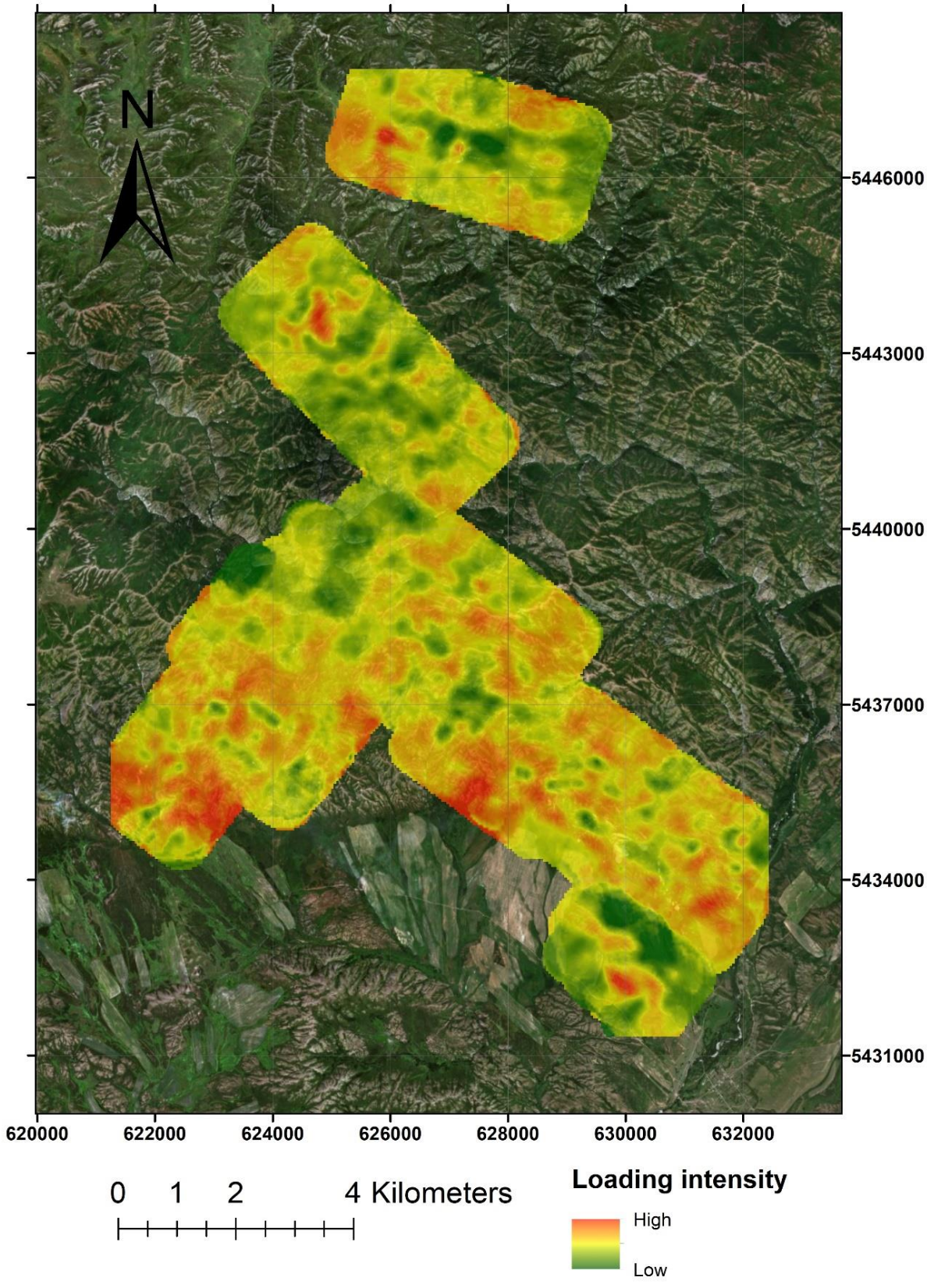

Figure 15. Factor 2. Preset of 5 factors were used. Kriging interpolation of the second factor with 500 meter coverage from data points. Factor 2 explains 14,264% of the total variance and includes positive loadings for Sr, Y, Fe, V, Sc, Ga, Co, Cr, Ni, Mg, Li, Zn, Cu and Na. Negative loadings for Ca, Rb and S.

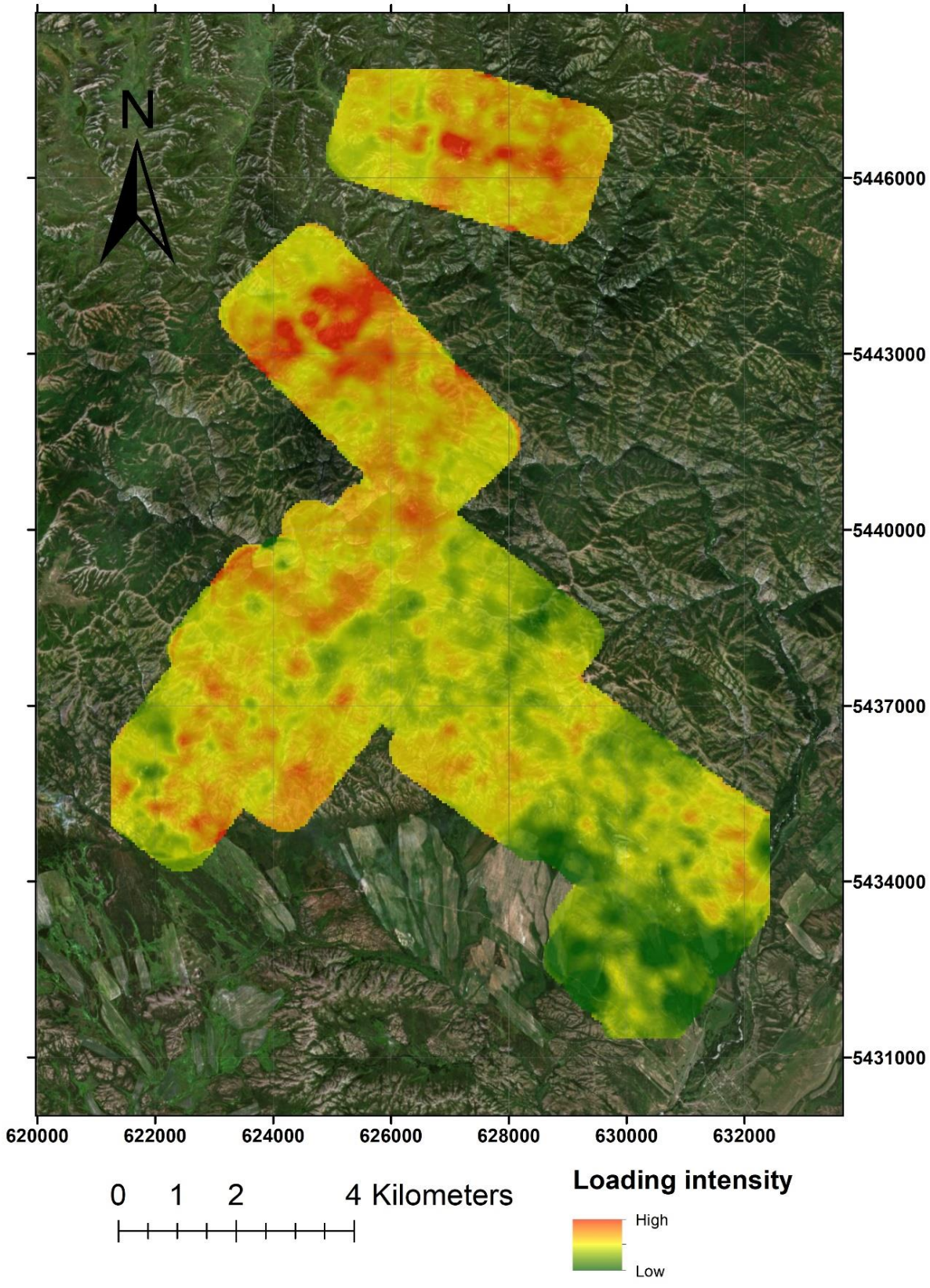

Figure 16. Factor 3. Preset of 5 factors were used. Kriging interpolation of the third factor with 500 meter coverage from data points. Factor 3 explains 10,947% of the total variance and includes positive loadings for Bi, Co, S, P, Mn, Zn, Cd, Cu, Mo, Ni and Sb. Negative loadings for Na and Sr.

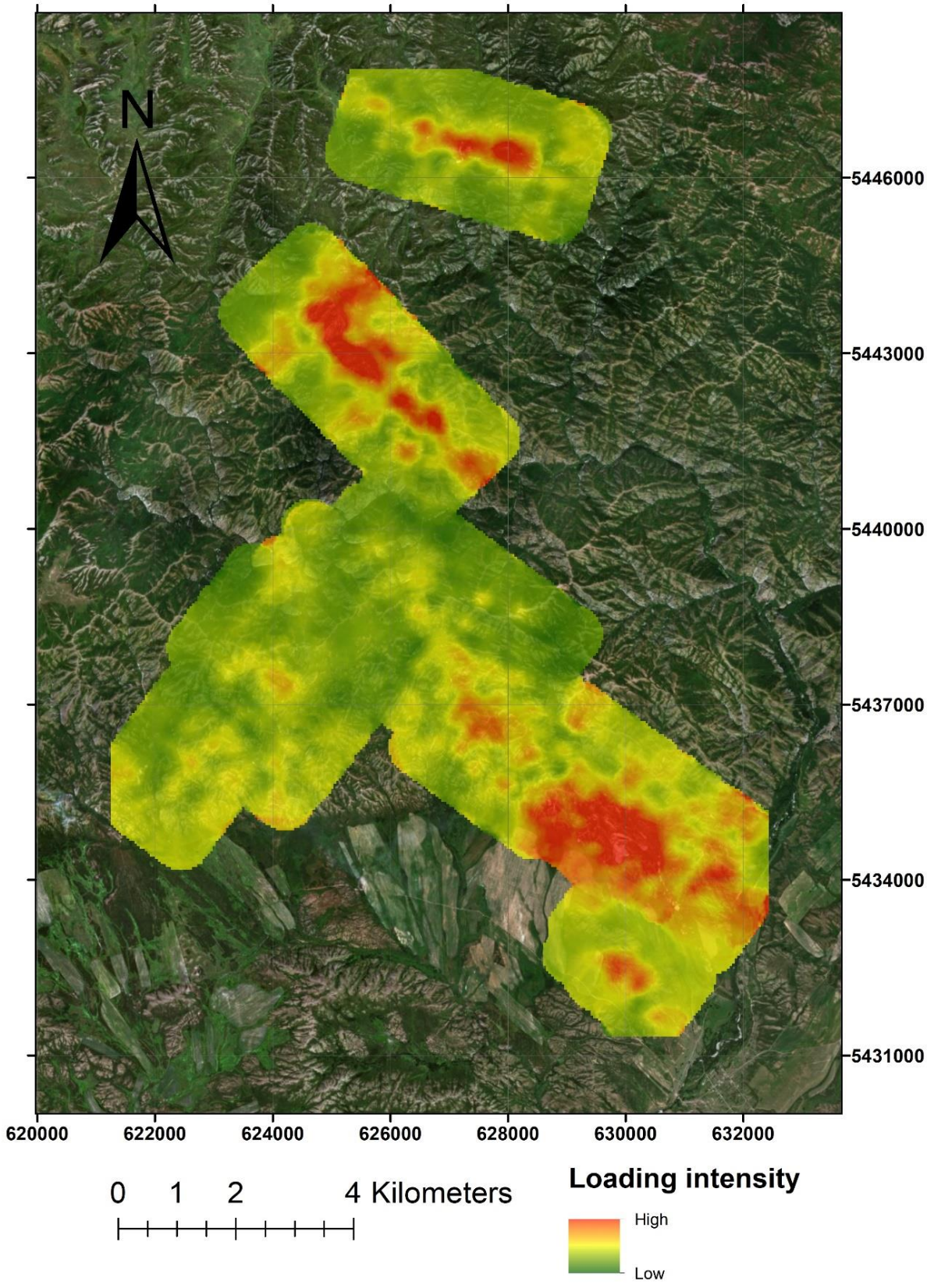

Figure 17. Factor 4. Preset of 5 factors were used. Kriging interpolation of the fourth factor with 500 meter coverage from data points. Factor 4 explains 6,431% of the total variance and includes positive loadings for As, Sb, Au, Zr, Sc, Mn, Mo, Cu, K and Ni. Negative loadings for Mg, Ta and Nb.

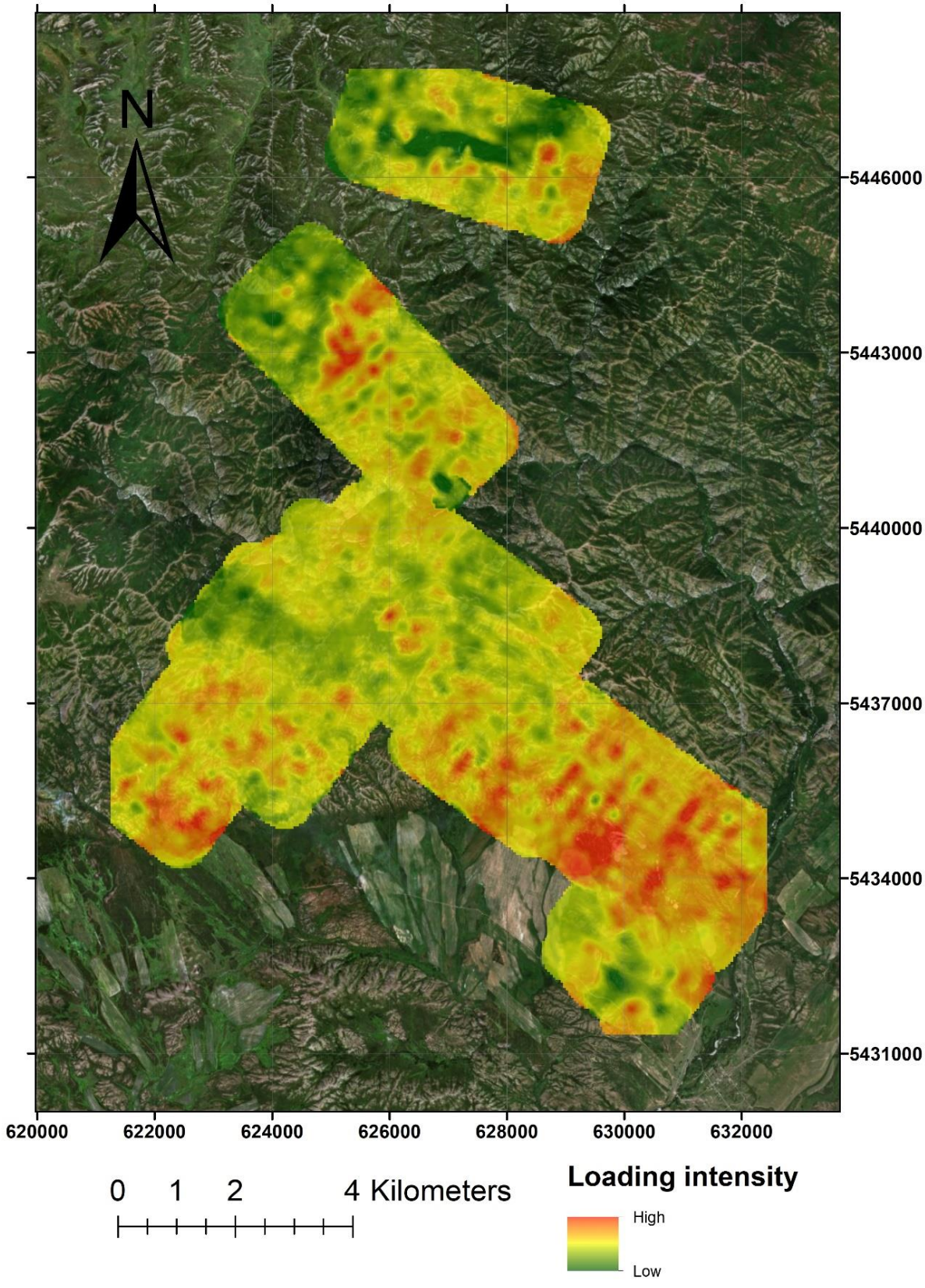

Figure 18. Factor 5. Preset of 5 factors were used. Kriging interpolation of the fifth factor with 500 meter coverage from data points. Factor 5 explains 4,142% of the total variance and includes positive loadings for Ca, Co, Cu, Pb and Sr. Negative loadings for Ba, Cr, and K.

With preset of six factors, as mentioned before, the first four factor maps are identical to their counterparts when using a preset of five factors. Therefore there is no need to present them again. Now starting from factor 5 (Figure 19.), a heavy loading in Brigadnoe can be observed. Smaller peaks of high loading are present in northern Svistun and in Belyi. In the center of Dzhumba project area there are shallow stripes of loading in northeast-southwest direction. Factor 6 (Figure 20.) has high loadings in the southeast and again they could be categorized as stripes following a northeast-southwest direction. Northwest has a relatively low loading intensity with the most noticeable singular peaks of higher loading being in east Brigadnoe and southwest Fedor-Ivanovskoe. As previously mentioned, map of factor 4 (Figure 21.) gained with the maximum likelihood method is identical to Figure 17. Hence, same observations apply to both.

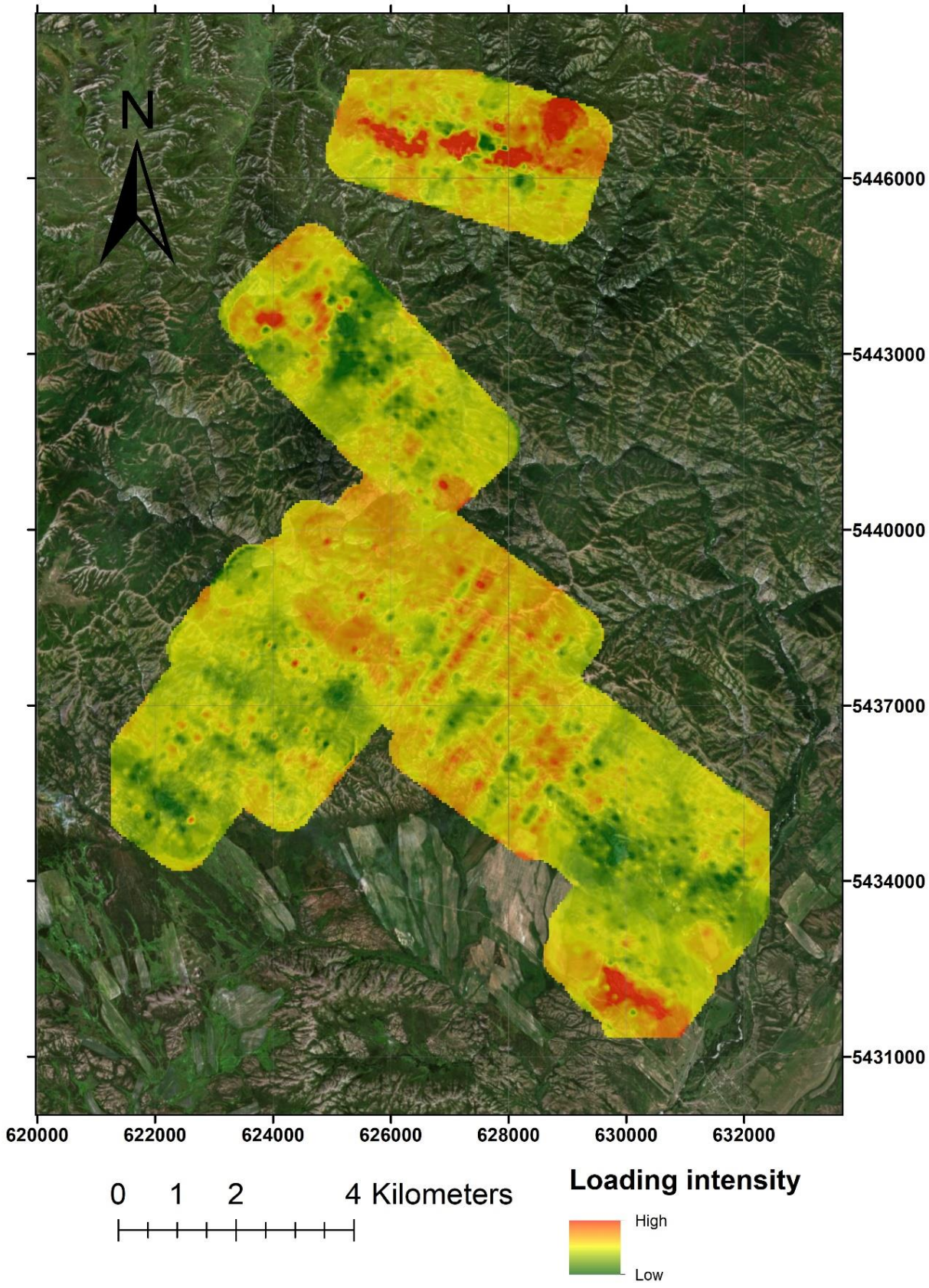

Figure 19. Factor 5. Preset of 6 factors were used. Kriging interpolation of the fifth factor with 500 meter coverage from data points. Factor 5 explains 4,142% of the total variance and includes positive loadings for Cr and Ni.

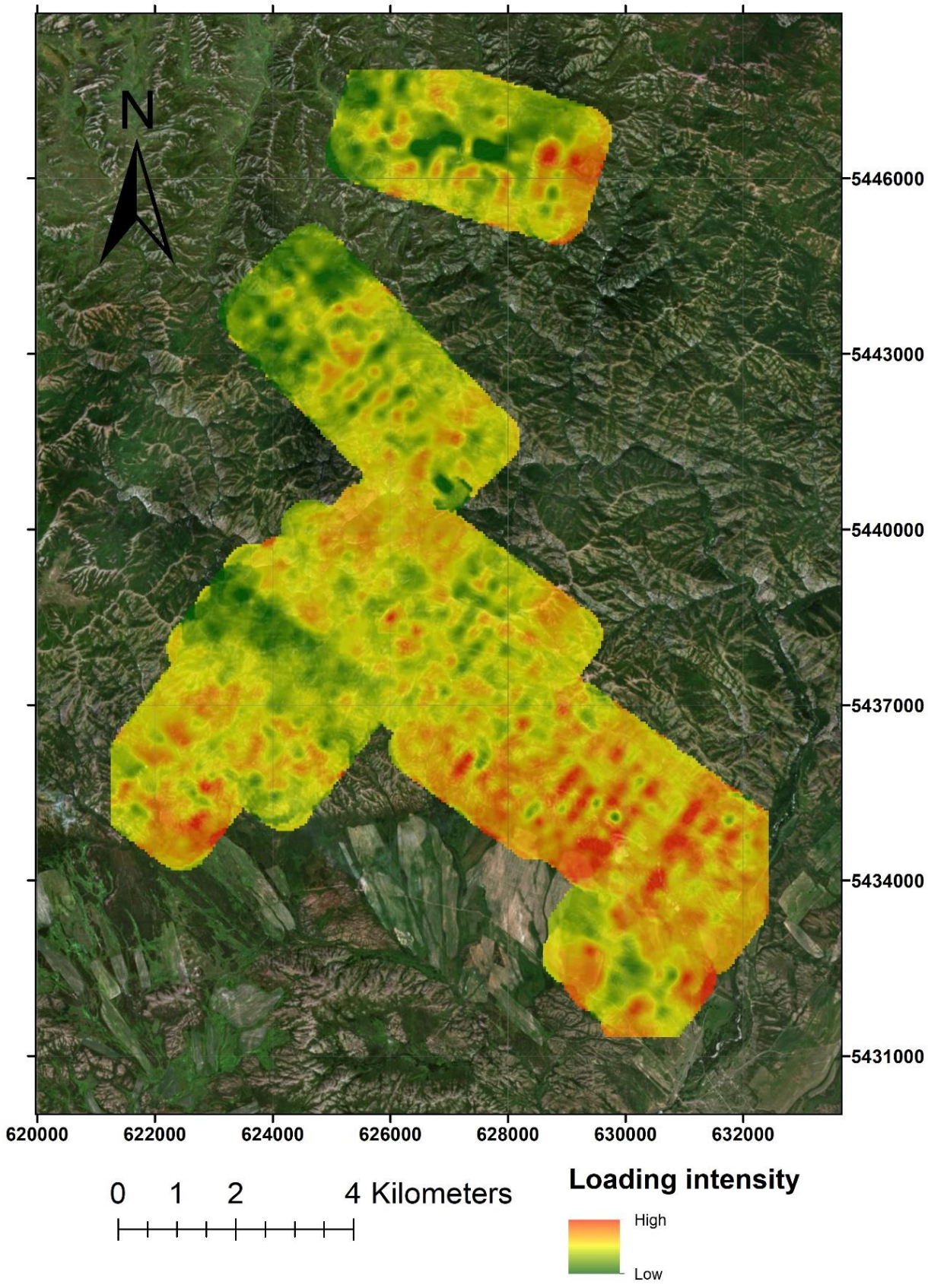

Figure 20. Factor 6. Preset of 6 factors were used. Kriging interpolation of the sixth factor with 500 meter coverage from data points. Factor 6 explains 3,079% of the total variance and includes positive loadings for Ca, Sr, S and Pb. Negative loadings for Ba and K.

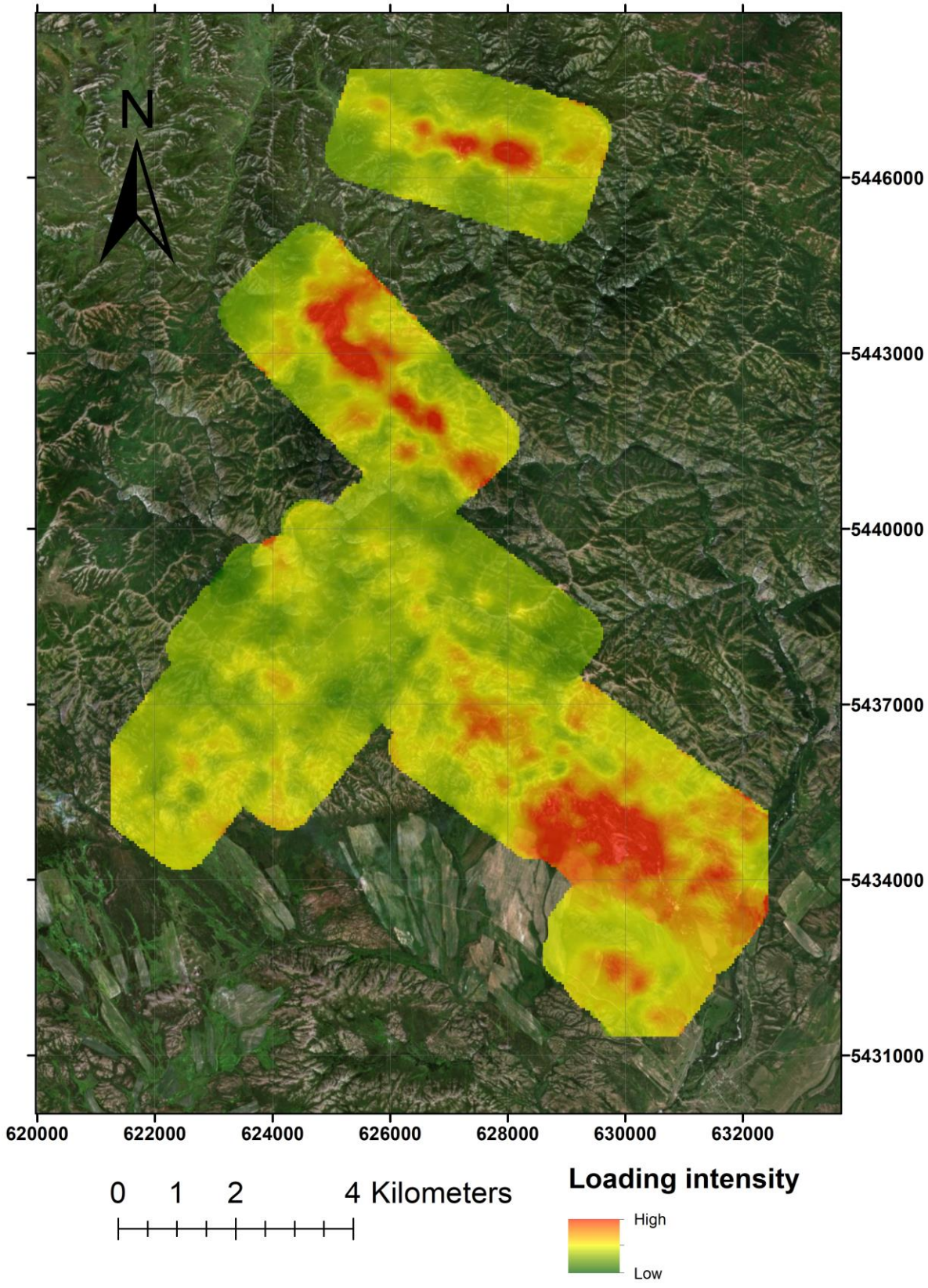

Figure 21. Factor 4. Kriging interpolation of the fourth factor using maximum likelihood factor analysis with 500 meter coverage from data points. Factor 4 explains 6,431% of the total variance and includes positive loadings for Au, As, Sb, Ni, Mo, Cu, Mn, Sc and Zr. Negative loadings for Nb, Ta and Mg.

5.5. Projection of factor 4 onto other data

In addition to plain factor analysis maps, it is interesting to compare the most exciting factor analysis map, factor 4, with other available data, for example the structural observations, strongest gold occurrences and alteration observations of the region. Figure 22. has structural observations on top of Figure 17. and it shows us the positions of shears, faults and veins that were observed during the fieldwork by Aurora Exploration Oy (ltd). Shears are marked as white, faults as blue and veins as red. All of them fit into the generated map quite well and conform the red areas of high loading. Veins are the most abundant structural formations and seem to follow the red areas most fittingly. Faults are not as plentiful as veins and they seem to be more dispersed from the red areas of high loading. Only two shears were observed, but they are right next to the red areas of high loading. The fourth factor seems to be the best fitting for structural correspondence out of all the different factors. Figure 23. shows the strongest gold occurrences overlain on Figure 17. The best fit would seem to be in Svistun and Dzhumba. The question of Fedor-Ivanovskoe is clearly seen as there is a robust gold occurrence but no loading for factor 4. Figure 24. has the intensities of ankerite alteration in a. and calcite alteration in b. shown on top of Figure 17. The alteration intensities conform the red areas of high loading surprisingly well. White dots of low alteration intensity are spread around the project area and the blue dots of strong alteration intensity are grouped in the red areas of high loading in Brigadnoe, Svistun, Dzhumba and Belyi. Southwest has a few points of strong alteration without a high loading for factor 4.

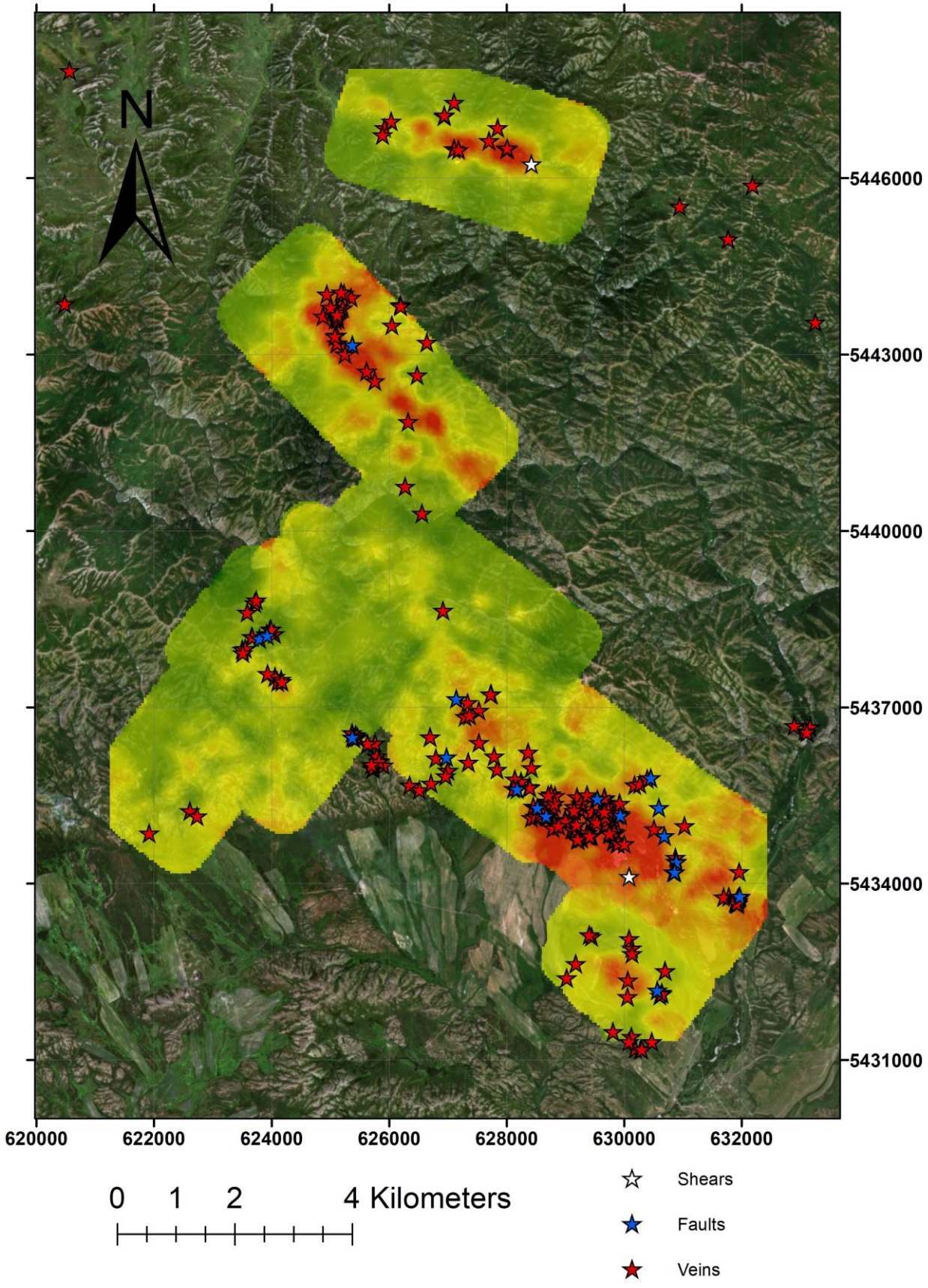

Figure 22. Shears, faults and veins that have been observed in the area overlain on the factor 4 map of Figure 17.

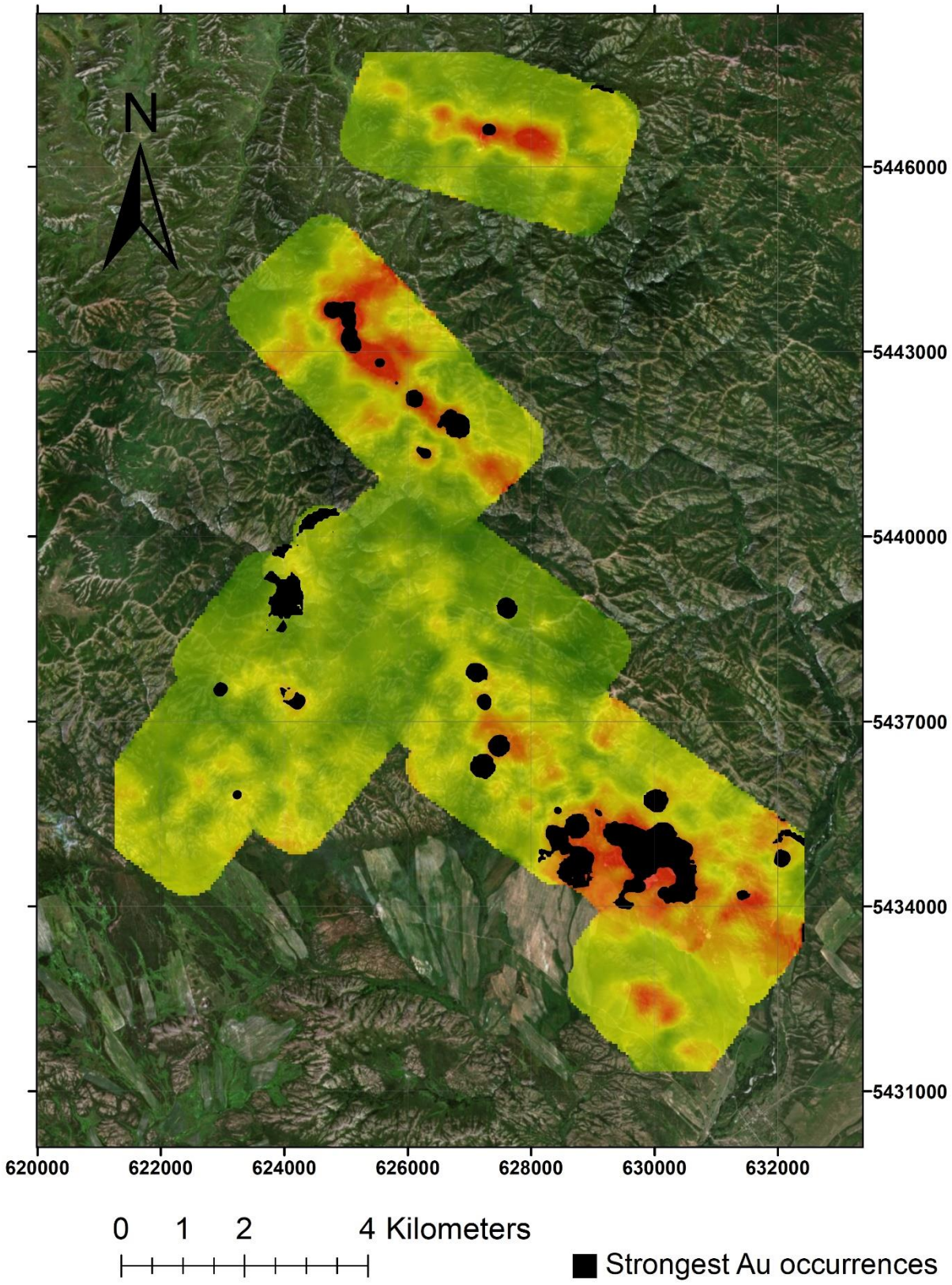

Figure 23. The strongest (over 0.09 ppm) gold occurrences overlain on the factor 4. map of Figure 17.

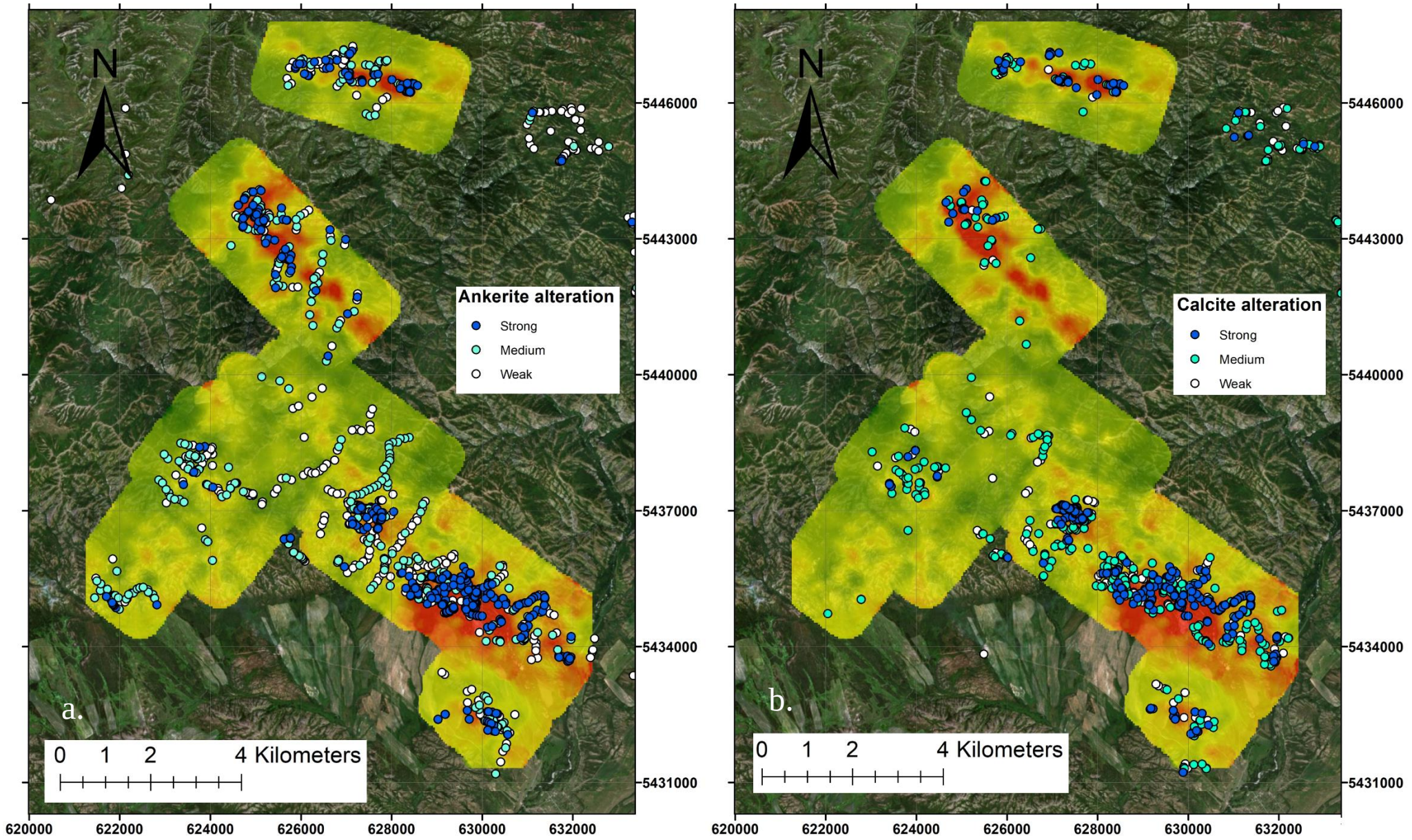

Figure 24. shows in a. ankerite alteration intensity and in b. calcite alteration intensity over factor 4 map of Figure 17.

6. DISCUSSION

6.1. Factor analysis as a tool to process data sets

The different factor analysis methods used in this study show that factor analysis is a viable method to process large data sets. Ag, Se and Te are the only elements that have no loadings in any of the factors. This is most likely due to the raw data of Ag, Se and Te being mostly below the detection limit. Their inclusion and impact on the analysis could be considered negligible. Loadings of all the other elements are satisfactory, however many exhibit cross-loading. In a perfect exploratory factor analysis, the elements should only load into one factor. Fortunately, most of the elements that do cross-load have a clear primary factor that they load onto that diverges by at least 0.2 compared to the secondary factor.

Comparing the map sets produced from the different preset of factors reveal that they are practically indistinguishable from each other. Even different analysis methods, maximum likelihood and proximal axis factoring, result in similar maps. The only obvious change is in the maps for factor 5. This coherence would indicate that the analysis is sound. Furthermore, all the different factors within a set are unique and give exclusive spatial distributions. This uniqueness and lack of identicality between the factors would point to a successful analysis.

6.2. Significance of elemental maps

Au, Sb and As maps generated from the raw data show certain differences. Antimony occurrence seems to be most homogenously widespread and dispersed of the three elements. Gold is the opposite with sharp and exact occurrences that do not radiate away from the center. Gold has high occurrences in Fedor-Ivanovskoe that As and Sb do not share. The background is darker green (low content) in Au and in As and Sb the background is light green or even yellow (medium content). However, they are still the most sharply outlined occurrences out of the other factor 4 elements. The most

homogenous distribution seems to be with manganese and nickel. The other elements fall somewhere in between the two extremes regarding distribution. Scandium is commonly concentrated more on mafic rocks (Eby, 1973), so the rise in Sc content could indicate more volcanoclastic components in the greywackes. It is also possible that Sc content represents the black shales (Vine and Tourtelot, 1970). High Mn content could indicate the carbonates in the area. Molybdenum, nickel and copper content could be related to black shales (Vine and Tourtelot, 1970). Similarity in the dispersion of Mn to Mo, Ni and Cu would suggest that Mn could be part of the black shales as well, maybe as a carbonate fraction (Vine and Tourtelot, 1970). Potassium has a poor correlation with Au. This could be explained by that there is no notable potassic alteration related to the gold mineralization.

Comparing which single element maps best match the single element map for gold, it would seem that As, Sb and Zr are the closest. As and Sb are common pathfinder elements for gold, but Zr is a slight surprise. Although the similarity between Au and Zr dispersion can be seen even in Table 4. where Zr has the highest loading in factor 4 after Au, As and Sb.

6.3. Factor 4 – the “gold factor”

The factor analysis produced one particularly interesting factor, namely factor 4. The elements grouped together in factor 4 with a preset of 5 factors were As, Sb, Au, Zr, Sc, Mn, Mo, Cu, K and Ni (Figure 17.). Arsenic, gold and antimony had the highest loadings for factor 4 and are clearly linked together. The correlation matrix in Table 9. found in the appendix section suggests a strong correlation between Au, As and Sb, so this was to be expected. Running the analysis with a preset of 6 factors gave very similar results with factor 4 loadings of As, Sb, Au, Zr, Sc, Mn, Cu and Ni (Table 5.). Also using a different extraction method, maximum likelihood, the same elements persisted (Figure 21.). Even if we take a look at the very first factor analysis (Table 3.) with no preset number of factors, factor 4 is still dominated with arsenic, gold and antimony.

Arsenic and antimony are both classically gold associated elements. Aurostibite ($AuSb_2$) has been found in eastern Kazakhstan (Kovalev et al., 2014). However, stibnite is the most common source of antimony in eastern Kazakhstan and is usually found in quartz-carbonate veins (Kalinin et al., 2015). When sulfur concentration is high, it can lead to stibnite and native gold assemblages, especially in black shale hosted gold deposits (Zhu et al., 2011). However, sulfur has not loaded into factor 4, so its concentration is not exceptionally high. When sulfur concentration is not high, Sb can still form from reducing $Sb(OH)_3$ which leads to the formation of native Sb and Au (Zheng et al., 2015; Zhu et al., 2011). Sb can also be found in arsenopyrite, pyrite, nickeline and tetrahedrite (Kalinin et al., 2015). Nickeline is one possibility that would explain the Ni loading for factor 4.

Moderate arsenic concentrations increase the solubility of gold in alkaline fluids (Zhu et al., 2011). According to Zhu et al. (2011), low sulfur content makes As to be the predominant Au carrier. This might be due to H_3AsO_3 being reduced by H_2S and H_2, and the H_2S and H_2 are coming from $Au(HS)_2^-$ (Garofalo and Ridley, 2014; Zheng et al., 2015). Therefore, the precipitation of As exhausts the HS_2 from $Au(HS)_2^-$, causing the precipitation of Au as well (Zheng et al., 2015). This fits factor 4 quite well as this is stated to happen in low sulfur conditions (Zheng et al., 2015).

As stated before, comparing the factor 4 maps produced from the different factor analyses show that they are virtually identical. Comparing them with the gold content map produced from the raw data however shows a few differences. Factor 4 shows high loadings in the north and in the southeast. The raw gold data in Figure 4. shows higher content in the southwest and a lesser content in the northernmost area with the southeast being relatively high in both maps. The raw data for arsenic in Figure 6. shows the same high content in the southeast as in factor 4. Arsenic content in the north however is quite low. Raw data for antimony in Figure 5. shows the best correlation with factor 4. out of Au, As and Sb.

Elements Zr, Sc, Mn, Mo, Cu, K and Ni have medium to low loadings in factor 4. Could some of these elements reside in hydrothermal graphite which is the core of the gold mineralization alteration zone in Dzhumba deposit? Proximal zones have abundant ankerite $Ca(Fe.Mg.Mn)(CO_3)_2$ zones which would explain the Mn loading but it does not

concur with the absence of Fe and Ca, let alone opposes the negative loading of Mg. The surprisingly high content of Zr could be explained by observing other lode-Au deposits, for example, hydrothermal zircons are paragenetically affiliated with vein quartz, carbonate, scheelite, tourmaline, mica, pyrite, and gold in the Norseman-Wiluna belt in Australia and in the Abitibi greenstone belt in Canada (Jiang et al., 2005). Cu and Mo are commonly associated with gold in porphyry Cu-Mo-Au deposits. Could there be some "graphitic" porphyry copper influence in the deposit?

When looking at the elements that are negatively loaded on factor 4, there are Ta, Nb and Mg. Both Ta and Nb are transition metals that belong to group 5 of the periodic table. Ta is enriched in pegmatites and peraluminous granites whereas Nb is enriched in alkali granites and bauxite (Mackay and Simandl, 2014; Pollard, 1989). This suits the interpretation of factor 4 representing gold mineralization as elements related to granitic origins, a different geological formation entirely, are negatively loaded. However, the strong negative loading of Mg is a slight surprise. This could be explained by Mg being present mainly in mafic rocks and therefore depleted in the non-mafic gold mineralization.

The elements in factor 4 suggest a hydrothermal origin, as Au, Cu, Mo, K and Mn are generally relatively soluble in near-neutral aqueous solutions (Ridley, 2013). These elements can form stable complexes such as $Au(HS)_2^-$ (Benning and Seward, 1996; Frimmel et al., 2005; Liu et al., 2014) and be present in aqueous solutions in higher concentrations, therefore found dominantly in hydrothermal deposits. However, following the principle of hard and soft acids, elements with different solute characteristics are unlikely to be enriched in the same hydrothermal system (Ridley, 2013). This means that hard metals (K^+, MoO^{3+} and As^{3+}) and soft metals (Au^+ and Cu^+) do not enrich in the same hydrothermal system (Crerar et al., 1985; Langmuir, 1997; Ridley, 2013) The presence of these elements in factor 4 would therefore mean that the elemental assemblage has come from different hydrothermal fluids and events.

Question arises, why the western side of the area has not been highlighted by factor 4 even though examining the single element gold map clearly shows a strong presence of gold there. This issue is best seen in Figure 23. where gold content is placed on top of factor 4. When examining the other elements in factor 4; As, Sb, Zr, Sc, Mn, Mo, Cu, K and Ni, their single element maps reveal that none of them have a strong occurrence in the western spot where gold is highlighted. This is the reason why factor 4 has neglected the western side almost completely. This however leads to another question, why gold is occurring here without the presence of other elements associated to it. Other factors that highlight this western spot are factor 1 and factor 3 although even they highlight this area quite faintly. Could this western gold occurrence be part of a separate mineralization that has different elemental composition than the factor 4 mineralization? Or perhaps it is a gold-only occurrence.

6.4. Significance of other factors 1, 2, 3, 5 and 6

Factor 1 (Figure 14.) seems to be comprised of elements that are commonly seen as trace elements. Especially Th, Nb, Ta, Rb, Tl, La, Bi, Ce, W, U, Y and Ga are not common major components in rocks, but here they have high loadings. The data suggests that these rocks formed from the same magmatic composition and it is reflected through the trace elements. Perhaps these trace elements were enriched in the remnant melt, which assimilated all the elements that did not fit into the more mafic minerals that crystallized first. The K loading would suggest a feldspar. Th, Nb, Ta, Y and Ga represent high-field-strength elements while La and Ce represent rare-earth elements. McCuaig & Kerrich (1998) state that these elements are typically unaffected by alteration. Loadings of Nb, Sn, Be and Li support a feldspar/granitic factor as these elements were found in higher concentrations in the granitoids of western Kalba belt (Safonova, 2014).

Factor 2 (Figure 15.) has very high loadings for iron and vanadium. These and most of the other elements Sr, Y, Sc, Ga, Co, Cr, Ni, Mg, Li, Zn, Cu and Na are transition elements. This could be the factor for mafic rocks. Or perhaps this represents black shales as Co, Cu, Zn, Ni, V and Cr are typically enriched in them (Västi, 2008). Sc and V are

transitional elements that are generally unaffected by alteration (McCuaig and Kerrich, 1998).

Factor 3 (Figure 16.) has the highest loading for P with Zn, Mn and Cd following suit. Bi, Co, S, Cu, Mo, Ni and Sb loadings are medium or low. S content here could mean a sulfide rich mafic mineral group. Another possibility is that this is related to the black shales, because P, S, Cu, Ni, Co and Mn contents are increased in graphite-bearing rocks (Dissanayake, 1993). Dissanayake (1993) found that these rocks transpired to be black shales, matching the lithology of Dzhumba.

Factor 5 is quite interesting as it is the only factor to show actually any kind of difference between the preset factor sets. With a preset of 5 factors, Ca, Co, Cu, Pb and Sr are found, but no element clearly stands out (Figure 18.). Pb has the highest loading and even that is under 0.5. The same elements are highlighted when using a preset of 6 factors with maximum likelihood method as seen in Table 6. Ca content could indicate the presence of carbonate rocks. Is this factor the indicator for the distal alteration zone which consists of calcite mineralization? Or even a proximal alteration zone with abundant calcite and ankerite? Although the presence of ankerite would mean that loadings for Fe, Mg or Mn should be observed. Pb, Co and Cu can be enriched in black shales (Västi, 2008). However, Pb, Co and Cu also poses an affinity for reaction with carbonates along with Sr (Kabata-Pendias, 2000). Therefore, factor 5 representing a calcite alteration would seem plausible. With a preset of 6 factors, using the principal axis factoring method, Cr and Ni are the only ones to have a loading (Figure 19.). When comparing element loadings for factor 5 and factor 6, it is as if they are rotated between principal axis factoring and maximum likelihood. Cr and Ni have a covariance between them and they are commonly found in basaltic rocks (Turekian, 1963). Considering the hydrothermal activity in the area, the more likely explanation is that they are mobile elements derived from Cr-muscovite and Ni-rich chlorite (McCuaig and Kerrich, 1998) or that they are part of the black shales (Västi, 2008).

Examining principal axis factoring results for factor 6, Figure 20. shows that it has loadings for Ca, Sr, S and Pb. These are similar what factor 5 showed with a preset of 5 factors with no loading rising above 0.5. Therefore, the same deduction applies to factor 6.

Factors 5 and 6 are, as stated before, rotated between principal axis factoring and maximum likelihood. Hence, Cr and Ni are highlighted for maximum likelihood method in factor 6 and for principal axis factoring in factor 5. Therefore the same deduction applies for maximum likelihood, Cr and Ni most likely represent black shales or hydrothermal activity.

6.5. The connection of structures and alteration

In Figure 22. all structural field observations: shears, faults and veins have been marked on top of the fourth factor map. Orogenic gold deposits are commonly structurally controlled (Goldfarb et al., 2001; Ridley, 2013), as gold is found in quartz veins and following host shear zones. Therefore, if the fourth factor represents mineralization, it would make sense for the veins, shears and faults to be present on the same area as well. Only a small group of faults and veins on the western side are inexplicable as there is seemingly no red trend under them. However, none of the different factors can clearly explain their appearance. Instead, the single element map for gold has a highlighted concentration beneath these structural details.

Figure 24. a. shows the alteration intensity of ankerite placed on top of factor 4 and Figure 24. b. shows the alteration intensity of calcite placed on top of factor 4. Both ankerite and calcite correlate well with factor 4 as the strongest alteration seems to exist inside the areas of high loading. This reinforces the idea of an orogenic gold deposit as ankerite and calcite are very typical minerals that are present as alteration haloes for orogenic gold deposits (Ridley, 2013).

6.6. Implications for Au exploration in the western Kalba belt

Gold exploration in the western Kalba belt could benefit from identifying pathfinder elements As, Sb, Zr, Sc, Mn, Mo, Cu, K and Ni that this factor analysis has grouped together to represent a gold mineralization. Also using the factor analysis method in new exploration targets around the western Kalba belt is a relatively cost effective and efficient way to identify possible gold mineralizations and pathfinder elements that are individual and descriptive for the specific exploration targets. Laying structural and alteration information on top of the newly generated factor maps may prove useful as well.

In the Dzhumba project, exploration could be targeted towards the areas highlighted by factor 4. Northern part of the area is the most promising prospect, because it is strongly highlighted by factor 4, but there is minimal amount of gold present when viewed as a single element gold map. Other elements related to gold are present and observed leaving the possibility of gold existing in the same area but not being observed in the regolith samples, possibly lying beneath the surface. This is supported by Figure 23. Also Fedor-Ivanovskoe could be explored more in order to clarify whether the gold anomaly there is related to another gold deposit type than in the rest of the Dzhumba project area, as it does not follow factor 4. Exploration could be expanded outwards and concentrated on areas that have high calcite and ankerite alteration with structural anomalies such as faults, shears and veins, as both alteration and structures seem abundant inside the halo of factor 4. When expanding the exploration areas, the search for elements that load intensely on factor 4 such as Sb, As and Zr could be as critical as searching for Au only.

7. CONCLUSIONS

The primary purpose of this thesis, the use of multivariate analysis to discover correlations with gold and other elements, was successful, as the factor analysis of Dzhumba project area provided 5 distinct factor groups, along with descriptive statistics and a correlation matrix. The elemental relations are understood more and factor analysis proved to be a viable geochemical exploration tool for the region. The original hypothesis was correct as the factor analysis was successful particularly in differentiating a clear gold

mineralization factor along with reasonable pathfinder elements. The data would suggest that the deposit type of the gold mineralization is an orogenic gold deposit.

Factor 1 represents granitic rocks by their feldspar and trace element content, factor 2 represents black shales with possible mafic rock constituents, factor 3 represents a sulfide rich mafic mineral group or graphitic rocks that are most likely the black shales, factor 4 represents the gold mineralization with high loadings on gold and its pathfinder elements arsenic and antimony, factor 5 possibly represents calcite alteration. Factor 4 is the main interest of this study. The most intense loadings for factor 4 are in Brigadnoe, Svistun and Dzhumba with a small peak in Belyi. The structural geology and alteration in the area conform to factor 4. Single element map for gold mostly corresponds to factor 4 for Svistun and Dzhumba, but Brigadnoe is represented with a small peak. However, gold has a major presence in Fedor-Ivanovskoe, which is absent from factor 4. Further exploration in Fedor-Ivanovskoe could be performed in order to clarify if this is due to an unrelated gold-only deposit or some other event. Possible future exploration in the area could benefit from factor 4 results, using As and Sb, or a combination of As, Sb, Zr, Sc, Mn, Mo, Cu, K and Ni as pathfinders for possible gold occurrences.

8. ACKNOWLEDGEMENTS

I would like to thank my supervisor Dr. Petri Peltonen for guidance in this thesis and for providing the essential data set, which is the backbone of this study. Also a big thank you goes to the Aurora Exploration Oy (ltd) field team for their work on collecting the regolith samples and noting field observations in the project area. Kazzinc Exploration Division is thanked for a permission to publish this thesis.

I thank my family and friends for encouragement and aid during these years at the university. Special thanks to my colleague students at the university who have provided peer support during the long days in the computer class.

9. REFERENCES

Benning, L. G. and Seward, T. M. 1996. Hydrosulphide complexing of Au (I) in hydrothermal solutions from 150–400 C and 500–1500 bar. Geochimica Et Cosmochimica Acta, 60, 1849-1871.

Bespayev, K. A., Mukayeva, A. E. and Grebennikov, S. I. 2018. General Patterns of Formation and Placement and Forecasting-Prospecting Criterias of Gold Ore Deposits in the Black Shale Strata of the West Kalba Belt of East Kazakhstan. News of the National Academy of Sciences of the Republic of Kazakhstan-Series of Geology and Technical Sciences 5, 172-183.

Crerar, D., Wood, S., Brantley, S. L. and Bocarsly, A. 1985. Chemical controls on solubility of ore-forming minerals in hydrothermal solutions. Canadian Mineralogist, 23, 333-352.

Dissanayake, C. 1993. Gold and other metals in graphite. Bitumens in Ore Deposits, 138-152.

DiStefano, C., Zhu, M. and Mindrila, D. 2009. Understanding and using factor scores: Considerations for the applied researcher. Practical assesment, research & evaluation, 14, 1-11.

Dyachkov, B., Mizernaya, M., Kuzmina, O., Zimanovskaya, N. and Oitseva, T. 2018. Tectonics and metallogeny of East Kazakhstan. IntechOpen, 67-84.

Eby, G. N. 1973. Scandium geochemistry of the Oka carbonatite complex, Oka, Quebec. American Mineralogist: Journal of Earth and Planetary Materials, 58, 819-825.

Frimmel, H. E., Groves, D. I., Kirk, J., Ruiz, J., Chesley, J. and Minter, W. E. 2005. The formation and preservation of the Witwatersrand goldfields, the world's largest gold province. Economic Geology, 100, 769-797.

Garofalo, P. S. and Ridley, J. R. 2014. Gold-Transporting Hydrothermal Fluids in the Earth's Crust: Geological Society, 47-49.

Goldfarb, R., Baker, T., Dube, B., Groves, D. I., Hart, C. J. and Gosselin, P. 2005. Distribution, character and genesis of gold deposits in metamorphic terranes. Society of Economic Geologists, 407-450

Goldfarb, R., Groves, D. and Gardoll, S. 2001. Orogenic gold and geologic time: a global synthesis. Ore Geology Reviews, 18, 1-75.

Healy, R. 2013. Integration of factor analysis and GIS in spatial modelling of the Dublin surge geochemical data set. Ireland: Dublin, 52 pp.

Jiang, S. Y., Wang, R. C., Xu, X. S. and Zhao, K. D. 2005. Mobility of high field strength elements (HFSE) in magmatic-, metamorphic-, and submarine-hydrothermal systems. Physics and Chemistry of the Earth, 30, 1020-1029.

Kabata-Pendias, A. 2000. Trace elements in soils and plants: CRC press, 56-57.

Kalinin, Y. A., Naumov, E. A., Borisenko, A. S., Kovalev, K. R. and Antropova, A. I. 2015. Spatial-temporal and genetic relationships between gold and antimony mineralization at gold-sulfide deposits of the Ob-Zaisan folded zone. Geology of Ore Deposits, 57, 157-171.

Kirmasov, A., Berezansky, A. and Kovalenko, D. 2017. Dzhumba Field Recon: Comments on exploration model and structural control, 94 pp.

Kovalev, K. R., Kalinin, Y. A., Naumov, E. A. and Myagkaya, M. K. 2014. Relationship of antimony with gold mineralization in the ore districts of Eastern Kazakhstan. Russian Geology and Geophysics, 55, 1170-1182.

Kovalev, K. R., Kalinin, Y. A., Naumov, E. A., Pirajno, F. and Borisenko, A. S. 2009. A mineralogical study of the Suzdal sediment-hosted gold deposit, Eastern Kazakhstan: Implications for ore genesis. Ore Geology Reviews, 35, 186-205.

Kuz'mina, O. N., D'yachkov, B. A., Vladimirov, A. G., Kirillov, M. V. and Redin, Y. O. 2013. Geology and mineralogy of East Kazakhstan gold-bearing jasperoids (by the example of the Baybura ore field). Russian Geology and Geophysics, 54, 1471-1483.

Langmuir, D. (1997). Aqueous environmental geochemistry. Prentice Hall, 600 pp.

Liu, W. H., Etschmann, B., Testemale, D., Hazemann, J. L., Rempel, K., Muller, H. and Brugger, J. 2014. Gold transport in hydrothermal fluids: Competition among the Cl-, Br-, HS- and NH3(aq) ligands. Chemical Geology, 376, 11-19.

Mackay, D. A. R. and Simandl, G. J. 2014. Geology, market and supply chain of niobium and tantalum-a review. Mineralium Deposita, 49, 1025-1047.

Marsh, E. E., Hart, C. J., Goldfarb, R. J., Allen, T. L., Roots, C. and Emond, D. 1998. Geology and geochemistry of the Clear Creek gold occurrences, Tombstone gold belt, central Yukon Territory. Yukon Exploration and Geology, 185-196.

McCuaig, T. C. and Kerrich, R. 1998. P-T-t-deformation-fluid characteristics of lode gold deposits: evidence from alteration systematics. Ore Geology Reviews, 12, 381-453.

Mizernaya, M., Dyachkov, B., Kusmina, O., Mizerny, A. and Oitseva, T. 2017. Main types of gold deposits of the eastern Kazakhstan. International Multidisciplinary Scientific GeoConference, 17, 299-306.

Mäkinen, J. 1989. Geochemical characteristics of svecokarelidic mafic-ultramafic intrusions associated with Ni-Cu occurrences in Finland. Geological survey of Finland bulletin 342, 109 pp.

Naden, J. and Shepherd, T. 1989. Role of methane and carbon dioxide in gold deposition. Nature, 342, 793-795.

Osborne, J. W. 2014. Best practices in exploratory factor analysis. CreateSpace Independent Publishing, 139 pp.

Osborne, J. W., Costello, A. B. and Kellow, J. T. 2008. Best practices in exploratory factor analysis. In: Osborne, J. W. (Ed.) Best practices in quantitative methods. SAGE, 86-99.

Peltonen, P. 2017. Aurora Exploration Field Season 2017 Report, 59 pp.

Peltonen, P. 2018. Aurora Exploration Field Season 2018 Report, 67 pp.

Pollard, P. J. 1989. Lanthanides, tantalum and niobium. Springer, 145-168.

Polymetalinternational. 2020. https://www.polymetalinternational.com/en/assets/where-we-operate/kyzyl/ site visited 4.1.2020.

Reimann, C., Filzmoser, P. and Garrett, R. G. 2002. Factor analysis applied to regional geochemical data: problems and possibilities. Applied Geochemistry, 17, 185-206.

Reis, A. P., Sousa, A. J., da Silva, E. F., Patinha, C. and Fonseca, E. C. 2004. Combining multiple correspondence analysis with factorial kriging analysis for geochemical mapping of the gold-silver deposit at Marrancos (Portugal). Applied Geochemistry, 19, 623-631.

Ridley, J. 2013. Ore deposit geology. Cambridge University Press, 92-238.

Safonova, I. 2014. The Russian-Kazakh Altai orogen: An overview and main debatable issues. Geoscience Frontiers, 5, 537-552.

Shapiro, S. S. and Wilk, M. B. 1965. An Analysis of Variance Test for Normality (Complete Samples). Biometrika, 52, 591.

Suhr, D. D. 2005. Principal component analysis vs. exploratory factor analysis. Paper presented at the Proceedings of the thirtieth annual SAS® users group international conference, 203-230.

Tripathi, V. S. 1979. Factor analysis in geochemical exploration. Journal of Geochemical Exploration, 11, 263-275.

Turekian, K. K. 1963. The Chromium and Nickel Distribution in Basaltic Rocks and Eclogites. Geochimica Et Cosmochimica Acta, 27, 835-846.

Vine, J. D. and Tourtelot, E. B. 1970. Geochemistry of black shale deposits; a summary report. Economic Geology, 65, 253-272.

Västi, K. 2008. Chemical composition of metamorphosed black shale and carbonaceous metasedimentary rocks at selected targets in the Vihanti area, Western Finland. Tutkimusraportti - Geologian Tutkimuskeskus, 1-22.

Zheng, B., Zhu, Y., An, F., Huang, Q.-y. and Qiu, T. 2015. As–Sb–Bi–Au mineralization in the Baogutu gold deposit, Xinjiang, NW China. Ore Geology Reviews, 69, 17-32.

Zhu, Y., An, F. and Tan, J. 2011. Geochemistry of hydrothermal gold deposits: a review. Geoscience Frontiers, 2, 367-374.

10. APPENDIX

Table 7. Shapiro-Wilk test showing that all elements have P value <0.05, so normality cannot be assumed.

	W	n	P
Au	0.189	3942	0.000
Ag	0.039	3942	0.000
Al	0.018	3942	0.000
As	0.252	3942	0.000
Ba	0.577	3942	0.000
Be	0.865	3942	0.000
Bi	0.740	3942	0.000
Ca	0.648	3942	0.000
Cd	0.661	3942	0.000
Ce	0.989	3942	0.000
Co	0.890	3942	0.000
Cr	0.463	3942	0.000
Cu	0.628	3942	0.000
Fe	0.995	3942	0.000
Ga	0.953	3942	0.000
Hg	0.004	3942	0.000
K	0.954	3942	0.000
La	0.965	3942	0.000
Li	0.877	3942	0.000
Mg	0.939	3942	0.000
Mn	0.595	3942	0.000
Mo	0.495	3942	0.000
Na	0.968	3942	0.000
Nb	0.963	3942	0.000
Ni	0.305	3942	0.000
P	0.959	3942	0.000
Pb	0.833	3942	0.000
Rb	0.977	3942	0.000
S	0.901	3942	0.000
Sb	0.366	3942	0.000
Sc	0.875	3942	0.000
Se	0.616	3942	0.000
Sn	0.603	3942	0.000
Sr	0.890	3942	0.000
Ta	0.954	3942	0.000
Te	0.111	3942	0.000

Table 7. continued

	W	n	P
Th	0.953	3942	0.000
Tl	0.812	3942	0.000
U	0.808	3942	0.000
V	0.973	3942	0.000
W	0.378	3942	0.000
Y	0.862	3942	0.000
Zn	0.790	3942	0.000
Zr	0.855	3942	0.000
logAu	0.738	3942	0.000
LogAg	0.049	3942	0.000
logAs	0.823	3942	0.000
logBa	0.883	3942	0.000
logBe	0.934	3942	0.000
logBi	0.901	3942	0.000
logCa	0.926	3942	0.000
logCd	0.894	3942	0.000
logCe	0.969	3942	0.000
logCo	0.987	3942	0.000
logCr	0.796	3942	0.000
logCu	0.926	3942	0.000
logFe	0.987	3942	0.000
logGa	0.917	3942	0.000
logK	0.929	3942	0.000
logLa	0.941	3942	0.000
logLi	0.942	3942	0.000
logMg	0.922	3942	0.000
logMn	0.915	3942	0.000
logMo	0.874	3942	0.000
logNa	0.956	3942	0.000
logNb	0.911	3942	0.000
logNi	0.792	3942	0.000
logP	0.997	3942	0.000
logPb	0.988	3942	0.000
logRb	0.911	3942	0.000
logS	0.994	3942	0.000
logSb	0.820	3942	0.000
logSc	0.932	3942	0.000
logSe	0.715	3942	0.000

Table 7. continued

	W	n	P
logSn	0.905	3942	0.000
logSr	0.964	3942	0.000
logTa	0.922	3942	0.000
logTe	0.117	3942	0.000
logTh	0.917	3942	0.000
logTl	0.829	3942	0.000
logU	0.938	3942	0.000
logV	0.981	3942	0.000
logW	0.619	3942	0.000
logY	0.913	3942	0.000
logZn	0.936	3942	0.000
logZr	0.936	3942	0.000

Table 8. Excerpt from the representative original chemical analysis, samples 3692 – 3703. All values in ppm.

N	3692	3693	2694	3695	3696	3697	3698	3699	3700	3701	3702	3703
Au	0.1885	0.0088	0.0037	0.0073	0.0068	0.0199	0.0047	0.0054	0.002	0.0038	0.0026	0.0054
Al	50000	50000	50000	50000	50000	50000	50000	50000	50000	50000	50000	50000
As	49	22	20	23	23	18	27	25	20	26	21	23
Ba	480	494	476	534	524	546	407	375	499	535	554	415
Be	1.8	2	1.7	2	1.9	1.8	1.6	1.5	1.9	1.9	2	1.8
Bi	0.25	0.33	0.28	0.32	0.31	0.29	0.29	0.28	0.35	0.37	0.39	0.27
Ca	9762	7209	11014	9213	9299	8318	15193	16732	10433	8487	11037	13063
Cd	0.4	0.5	0.4	0.3	0.4	0.5	0.5	0.5	0.4	0.5	0.7	0.4
Ce	63	60	58	69	68	64	54	51	63	65	66	60
Co	37.2	24	23.7	20	19.2	23.5	15.4	14.2	36.2	28.4	34.7	18.4
Cr	58	69	74	72	73	70	65	61	68	77	75	67
Cu	52	39	35	33	32	33	45	48	48	40	47	33
Fe	41356	41028	43158	37990	37681	39747	31146	29306	43158	41729	42362	34308
Ga	21.6	20.3	21	19.8	19.5	21.1	16.9	15.8	20	21.2	20.5	18.7
Ge	0.2	0.2	0.2	0.2	0.2	0.2	0.2	0.2	0.2	0.2	0.2	0.2
Hg	1	1	1	1	1	1	1	1	1	1	1	1
K	23332	19067	21140	21352	21125	21398	17155	16100	20208	21926	21329	17618
La	25.6	28.7	25.5	31	30.9	26.9	24.9	24.3	26.5	28.4	29	27.3
Li	30	36	35	33	33	33	26	25	37	37	38	29
Mg	11154	11404	11653	10288	10182	10855	8704	8396	11200	11239	11305	9894
Mn	1496	1367	1408	1242	1228	1352	909	827	1702	1315	1470	687
Mo	1.6	1.4	1.4	1.3	1.2	1.1	1.3	0.9	1.8	1.5	1.3	0.8
Na	9371	10684	13569	13199	13222	12586	9996	10272	10466	11716	12035	13825

Table 8. continued

N	3692	3693	2694	3695	3696	3697	3698	3699	3700	3701	3702	3703
Nb	7.65	9.41	9.02	10.64	10.34	9.89	8.24	7.99	10.16	10.06	10.56	9.24
Ni	34	34	37	37	35	37	34	35	41	37	44	34
P	1217	1451	1287	909	893	1020	1354	1223	1880	1200	1383	1042
Pb	32	35	45	46	50	61	40	31	47	40	45	37
Rb	87	92	87	90	90	91	93	83	101	94	102	88
Re	0.01	0.01	0.01	0.01	0.01	0.01	0.01	0.01	0.01	0.01	0.01	0.01
S	697	629	629	440	443	483	1181	1410	975	632	684	799
Sb	1.7	1.3	1.1	1.3	1.2	1.2	1.1	1	1.2	1.3	1.3	1
Sc	16	15	15	15	14	15	12	12	15	15	15	13
Se	1.5	1.5	1.5	1.5	1.5	1.5	2	2	2	1.5	1.5	2
Sn	1.8	2.1	2.1	2.2	2.2	2.1	1.9	1.8	2.2	2.4	2.3	2
Sr	135	155	206	162	162	180	170	180	173	163	178	209
Ta	0.54	0.7	0.66	0.82	0.79	0.74	0.65	0.6	0.72	0.76	0.78	0.67
Te	5	5	5	5	5	5	5	5	5	5	5	5
Th	7.54	8.97	8.59	11.34	11.14	9.65	9.18	8.89	10.19	10.58	10.74	9.15
Ti	1000	1000	1000	1000	1000	1000	1000	1000	1000	1000	1000	1000
Tl	0.4	0.5	0.4	0.5	0.5	0.5	0.5	0.4	0.5	0.5	0.6	0.5
U	2.54	2.75	2.59	2.47	2.42	2.92	5.31	3.26	3.04	2.62	3.39	3.62
V	114	107	113	95	94	103	79	74	97	103	102	89
W	2	2	1	2	2	2	1	2	2	2	2	1
Y	19.1	20.8	18.8	20.7	20.4	18.7	16.6	17.5	19.4	18.5	20.1	19.2
Zn	90	104	95	81	81	101	87	84	113	114	135	77
Zr	76	78	76	90	90	84	67	67	77	83	84	73

Table 9. a-d Correlation matrix of log transformed data.

Table 9. a

	Au	Ag	As	Ba	Be	Bi	Ca	Cd	Ce	Co
Au	1.000	0.002	0.742	-0.033	0.062	-0.103	0.036	-0.076	-0.124	0.064
Ag	0.002	1.000	-0.010	0.015	-0.010	-0.010	0.000	0.023	-0.022	0.021
As	0.742	-0.010	1.000	0.009	0.098	-0.091	-0.053	-0.002	-0.070	0.243
Ba	-0.033	0.015	0.009	1.000	0.261	0.313	-0.475	0.086	0.347	-0.138
Be	0.062	-0.010	0.098	0.261	1.000	0.374	-0.272	0.036	0.346	0.143
Bi	-0.103	-0.010	-0.091	0.313	0.374	1.000	-0.444	0.215	0.589	0.023
Ca	0.036	0.000	-0.053	-0.475	-0.272	-0.444	1.000	0.035	-0.439	-0.050
Cd	-0.076	0.023	-0.002	0.086	0.036	0.215	0.035	1.000	0.037	0.174
Ce	-0.124	-0.022	-0.070	0.347	0.346	0.589	-0.439	0.037	1.000	0.023
Co	0.064	0.021	0.243	-0.138	0.143	0.023	-0.050	0.174	0.023	1.000
Cr	-0.049	0.029	0.004	0.354	0.153	0.144	-0.288	-0.057	0.214	-0.038
Cu	0.219	0.021	0.332	-0.253	0.042	0.139	0.008	0.264	-0.069	0.526
Fe	0.090	0.032	0.246	0.035	0.157	-0.031	-0.212	-0.117	0.024	0.611
Ga	0.138	0.022	0.203	0.217	0.406	0.238	-0.378	-0.182	0.247	0.366

Table 9. a continued

	Au	Ag	As	Ba	Be	Bi	Ca	Cd	Ce	Co
K	0.131	0.012	0.133	0.527	0.321	0.398	-0.490	-0.046	0.376	-0.108
La	-0.083	-0.017	-0.051	0.338	0.508	0.579	-0.416	0.108	0.712	-0.067
Li	0.074	-0.026	0.123	0.132	0.287	0.377	-0.415	-0.098	0.239	0.136
Mg	-0.304	0.025	-0.277	-0.009	0.066	-0.059	-0.054	-0.111	0.077	0.330
Mn	0.161	0.002	0.273	-0.056	0.120	0.348	-0.190	0.271	0.093	0.489
Mo	0.135	0.052	0.244	0.103	0.145	0.281	-0.202	0.352	0.114	0.413
Na	0.024	0.015	0.008	-0.117	-0.012	-0.348	0.087	-0.426	-0.094	0.164
Nb	-0.217	0.016	-0.288	0.453	0.478	0.670	-0.430	-0.041	0.637	-0.123
Ni	0.143	0.019	0.235	0.087	0.141	0.248	-0.151	0.206	0.150	0.293
P	-0.081	-0.009	-0.028	-0.121	-0.147	0.119	0.066	0.520	-0.048	0.220
Pb	0.058	0.001	0.151	0.010	0.289	0.287	0.044	0.289	0.227	0.186
Rb	-0.082	0.013	-0.154	0.440	0.391	0.654	-0.427	0.097	0.579	-0.325
S	0.043	-0.016	0.017	-0.371	-0.271	-0.130	0.598	0.341	-0.327	-0.041
Sb	0.548	-0.004	0.686	-0.009	0.169	0.122	-0.097	0.139	0.004	0.307
Sc	0.248	0.007	0.407	-0.051	0.074	-0.122	-0.214	-0.182	-0.050	0.465
Se	-0.070	-0.012	-0.060	0.055	-0.055	0.089	-0.011	0.176	-0.021	0.038
Sn	-0.105	0.042	-0.135	0.368	0.254	0.593	-0.425	0.045	0.452	-0.007
Sr	0.042	-0.018	-0.004	-0.262	-0.153	-0.406	0.465	-0.258	-0.299	0.201
Ta	-0.235	0.027	-0.304	0.447	0.450	0.665	-0.406	-0.015	0.581	-0.182
Te	-0.016	0.015	-0.023	0.050	0.010	-0.042	0.012	-0.045	0.047	-0.028
Th	-0.141	0.012	-0.163	0.428	0.476	0.710	-0.405	0.061	0.693	-0.223
Tl	-0.076	0.027	-0.109	0.525	0.436	0.688	-0.430	0.128	0.503	-0.194
U	-0.165	0.050	-0.171	0.204	0.319	0.480	-0.302	0.179	0.369	0.057
V	0.112	0.021	0.204	0.075	0.060	-0.136	-0.210	-0.196	-0.040	0.468
W	0.131	0.002	0.091	0.304	0.289	0.440	-0.302	0.061	0.316	-0.099
Y	-0.064	0.016	-0.014	0.149	0.278	0.341	-0.219	0.059	0.430	0.115
Zn	0.017	0.018	0.092	0.165	0.141	0.365	-0.228	0.408	0.236	0.367
Zr	0.247	0.022	0.283	0.345	0.343	0.435	-0.439	-0.052	0.344	-0.060

Table 9. b

	Cr	Cu	Fe	Ga	K	La	Li	Mg	Mn	Mo
Au	-0.049	0.219	0.090	0.138	0.131	-0.083	0.074	-0.304	0.161	0.135
Ag	0.029	0.021	0.032	0.022	0.012	-0.017	-0.026	0.025	0.002	0.052
As	0.004	0.332	0.246	0.203	0.133	-0.051	0.123	-0.277	0.273	0.244
Ba	0.354	-0.253	0.035	0.217	0.527	0.338	0.132	-0.009	-0.056	0.103
Be	0.153	0.042	0.157	0.406	0.321	0.508	0.287	0.066	0.120	0.145
Bi	0.144	0.139	-0.031	0.238	0.398	0.579	0.377	-0.059	0.348	0.281
Ca	-0.288	0.008	-0.212	-0.378	-0.490	-0.416	-0.415	-0.054	-0.190	-0.202
Cd	-0.057	0.264	-0.117	-0.182	-0.046	0.108	-0.098	-0.111	0.271	0.352
Ce	0.214	-0.069	0.024	0.247	0.376	0.712	0.239	0.077	0.093	0.114
Co	-0.038	0.526	0.611	0.366	-0.108	-0.067	0.136	0.330	0.489	0.413
Cr	1.000	-0.207	0.287	0.207	0.250	0.202	0.200	0.278	-0.140	-0.075

Table 9. b continued

	Cr	Cu	Fe	Ga	K	La	Li	Mg	Mn	Mo
Cu	-0.207	1.000	0.305	0.130	-0.072	-0.023	0.189	-0.052	0.645	0.496
Fe	0.287	0.305	1.000	0.616	0.082	-0.070	0.309	0.464	0.260	0.239
Ga	0.207	0.130	0.616	1.000	0.357	0.198	0.412	0.239	0.140	0.200
K	0.250	-0.072	0.082	0.357	1.000	0.417	0.237	-0.090	0.112	0.079
La	0.202	-0.023	-0.070	0.198	0.417	1.000	0.272	-0.020	0.101	0.161
Li	0.200	0.189	0.309	0.412	0.237	0.272	1.000	0.139	0.340	0.152
Mg	0.278	-0.052	0.464	0.239	-0.090	-0.020	0.139	1.000	-0.147	-0.161
Mn	-0.140	0.645	0.260	0.140	0.112	0.101	0.340	-0.147	1.000	0.553
Mo	-0.075	0.496	0.239	0.200	0.079	0.161	0.152	-0.161	0.553	1.000
Na	0.084	-0.119	0.386	0.321	-0.115	-0.150	0.010	0.362	-0.225	-0.231
Nb	0.338	-0.324	-0.060	0.306	0.490	0.617	0.244	0.158	-0.052	-0.048
Ni	0.476	0.425	0.305	0.126	0.206	0.213	0.295	-0.003	0.416	0.314
P	-0.171	0.283	-0.133	-0.304	-0.162	-0.075	-0.065	-0.140	0.430	0.323
Pb	-0.093	0.236	0.085	0.080	0.051	0.274	0.010	0.001	0.275	0.241
Rb	0.246	-0.273	-0.324	0.117	0.601	0.626	0.137	-0.171	-0.015	0.025
S	-0.356	0.176	-0.426	-0.538	-0.406	-0.234	-0.253	-0.300	0.151	0.139
Sb	-0.012	0.511	0.248	0.273	0.107	0.083	0.318	-0.329	0.475	0.426
Sc	0.296	0.371	0.747	0.548	0.077	-0.062	0.331	0.161	0.266	0.211
Se	0.020	0.081	-0.017	-0.048	-0.012	0.130	0.028	-0.003	0.084	0.171
Sn	0.276	-0.072	0.028	0.302	0.397	0.516	0.266	0.037	0.104	0.173
Sr	-0.186	0.029	0.285	0.145	-0.358	-0.399	-0.153	0.163	-0.101	-0.130
Ta	0.351	-0.348	-0.107	0.205	0.465	0.599	0.215	0.146	-0.076	-0.054
Te	0.106	-0.090	0.032	0.021	0.038	0.011	0.074	0.073	-0.041	-0.032
Th	0.273	-0.235	-0.200	0.154	0.474	0.754	0.217	-0.056	0.014	0.041
Tl	0.299	-0.151	-0.172	0.206	0.542	0.588	0.289	-0.124	0.074	0.169
U	0.144	0.065	0.023	0.225	0.105	0.414	0.116	-0.005	0.107	0.285
V	0.305	0.204	0.841	0.607	0.100	-0.117	0.310	0.485	0.088	0.180
W	0.224	-0.120	-0.035	0.172	0.393	0.343	0.240	-0.146	0.079	0.063
Y	0.257	0.188	0.253	0.345	0.250	0.563	0.183	0.130	0.091	0.158
Zn	0.111	0.431	0.307	0.154	0.141	0.073	0.219	-0.016	0.486	0.431
Zr	0.138	0.190	0.079	0.363	0.560	0.462	0.484	-0.314	0.295	0.252

Table 9. c

	Na	Nb	Ni	P	Pb	Rb	S	Sb	Sc	Se	Sn
Au	0.024	-0.217	0.143	-0.081	0.058	-0.082	0.043	0.548	0.248	-0.070	-0.105
Ag	0.015	0.016	0.019	-0.009	0.001	0.013	-0.016	-0.004	0.007	-0.012	0.042
As	0.008	-0.288	0.235	-0.028	0.151	-0.154	0.017	0.686	0.407	-0.060	-0.135
Ba	-0.117	0.453	0.087	-0.121	0.010	0.440	-0.371	-0.009	-0.051	0.055	0.368
Be	-0.012	0.478	0.141	-0.147	0.289	0.391	-0.271	0.169	0.074	-0.055	0.254
Bi	-0.348	0.670	0.248	0.119	0.287	0.654	-0.130	0.122	-0.122	0.089	0.593
Ca	0.087	-0.430	-0.151	0.066	0.044	-0.427	0.598	-0.097	-0.214	-0.011	-0.425
Cd	-0.426	-0.041	0.206	0.520	0.289	0.097	0.341	0.139	-0.182	0.176	0.045

Table 9. c continued

	Na	Nb	Ni	P	Pb	Rb	S	Sb	Sc	Se	Sn
Ce	-0.094	0.637	0.150	-0.048	0.227	0.579	-0.327	0.004	-0.050	-0.021	0.452
Co	0.164	-0.123	0.293	0.220	0.186	-0.325	-0.041	0.307	0.465	0.038	-0.007
Cr	0.084	0.338	0.476	-0.171	-0.093	0.246	-0.356	-0.012	0.296	0.020	0.276
Cu	-0.119	-0.324	0.425	0.283	0.236	-0.273	0.176	0.511	0.371	0.081	-0.072
Fe	0.386	-0.060	0.305	-0.133	0.085	-0.324	-0.426	0.248	0.747	-0.017	0.028
Ga	0.321	0.306	0.126	-0.304	0.080	0.117	-0.538	0.273	0.548	-0.048	0.302
K	-0.115	0.490	0.206	-0.162	0.051	0.601	-0.406	0.107	0.077	-0.012	0.397
La	-0.150	0.617	0.213	-0.075	0.274	0.626	-0.234	0.083	-0.062	0.130	0.516
Li	0.010	0.244	0.295	-0.065	0.010	0.137	-0.253	0.318	0.331	0.028	0.266
Mg	0.362	0.158	-0.003	-0.140	0.001	-0.171	-0.300	-0.329	0.161	-0.003	0.037
Mn	-0.225	-0.052	0.416	0.430	0.275	-0.015	0.151	0.475	0.266	0.084	0.104
Mo	-0.231	-0.048	0.314	0.323	0.241	0.025	0.139	0.426	0.211	0.171	0.173
Na	1.000	-0.078	-0.153	-0.430	-0.067	-0.356	-0.372	-0.091	0.344	-0.114	-0.169
Nb	-0.078	1.000	0.059	-0.167	0.052	0.790	-0.406	-0.198	-0.196	-0.044	0.659
Ni	-0.153	0.059	1.000	0.079	0.097	0.083	-0.074	0.413	0.357	0.100	0.192
P	-0.430	-0.167	0.079	1.000	0.100	-0.011	0.581	0.047	-0.130	0.186	-0.046
Pb	-0.067	0.052	0.097	0.100	1.000	0.068	0.104	0.228	-0.047	0.028	-0.062
Rb	-0.356	0.790	0.083	-0.011	0.068	1.000	-0.178	-0.104	-0.311	0.035	0.565
S	-0.372	-0.406	-0.074	0.581	0.104	-0.178	1.000	0.057	-0.324	0.201	-0.267
Sb	-0.091	-0.198	0.413	0.047	0.228	-0.104	0.057	1.000	0.415	0.028	0.030
Sc	0.344	-0.196	0.357	-0.130	-0.047	-0.311	-0.324	0.415	1.000	-0.020	0.008
Se	-0.114	-0.044	0.100	0.186	0.028	0.035	0.201	0.028	-0.020	1.000	0.154
Sn	-0.169	0.659	0.192	-0.046	-0.062	0.565	-0.267	0.030	0.008	0.154	1.000
Sr	0.628	-0.319	-0.194	-0.163	-0.004	-0.527	-0.022	-0.057	0.143	-0.096	-0.340
Ta	-0.097	0.907	0.062	-0.154	0.121	0.751	-0.365	-0.229	-0.237	0.027	0.602
Te	0.035	0.011	0.057	0.009	-0.017	0.000	0.008	-0.015	0.000	-0.009	0.004
Th	-0.202	0.818	0.115	-0.106	0.216	0.820	-0.236	-0.065	-0.230	0.045	0.606
Tl	-0.334	0.711	0.225	-0.078	0.087	0.758	-0.218	0.038	-0.172	0.102	0.616
U	-0.212	0.490	0.114	0.111	0.078	0.430	-0.165	-0.048	-0.058	0.074	0.449
V	0.450	-0.108	0.239	-0.232	-0.047	-0.355	-0.452	0.207	0.734	0.017	0.020
W	-0.220	0.470	0.162	-0.019	0.011	0.491	-0.142	0.128	-0.047	0.041	0.395
Y	0.010	0.370	0.315	-0.154	0.074	0.282	-0.269	0.097	0.330	0.101	0.325
Zn	-0.252	0.114	0.420	0.462	0.149	0.098	0.024	0.243	0.231	0.027	0.245
Zr	-0.127	0.312	0.305	-0.170	0.073	0.358	-0.275	0.433	0.260	0.017	0.394

Table 9. d

	Sr	Ta	Te	Th	Tl	U	V	W	Y	Zn	Zr
Au	0.042	-0.235	-0.016	-0.141	-0.076	-0.165	0.112	0.131	-0.064	0.017	0.247
Ag	-0.018	0.027	0.015	0.012	0.027	0.050	0.021	0.002	0.016	0.018	0.022
As	-0.004	-0.304	-0.023	-0.163	-0.109	-0.171	0.204	0.091	-0.014	0.092	0.283
Ba	-0.262	0.447	0.050	0.428	0.525	0.204	0.075	0.304	0.149	0.165	0.345
Be	-0.153	0.450	0.010	0.476	0.436	0.319	0.060	0.289	0.278	0.141	0.343
Bi	-0.406	0.665	-0.042	0.710	0.688	0.480	-0.136	0.440	0.341	0.365	0.435
Ca	0.465	-0.406	0.012	-0.405	-0.430	-0.302	-0.210	-0.302	-0.219	-0.228	-0.439

Table 9. d continued

	Sr	Ta	Te	Th	Tl	U	V	W	Y	Zn	Zr
Cd	-0.258	-0.015	-0.045	0.061	0.128	0.179	-0.196	0.061	0.059	0.408	-0.052
Ce	-0.299	0.581	0.047	0.693	0.503	0.369	-0.040	0.316	0.430	0.236	0.344
Co	0.201	-0.182	-0.028	-0.223	-0.194	0.057	0.468	-0.099	0.115	0.367	-0.060
Cr	-0.186	0.351	0.106	0.273	0.299	0.144	0.305	0.224	0.257	0.111	0.138
Cu	0.029	-0.348	-0.090	-0.235	-0.151	0.065	0.204	-0.120	0.188	0.431	0.190
Fe	0.285	-0.107	0.032	-0.200	-0.172	0.023	0.841	-0.035	0.253	0.307	0.079
Ga	0.145	0.205	0.021	0.154	0.206	0.225	0.607	0.172	0.345	0.154	0.363
K	-0.358	0.465	0.038	0.474	0.542	0.105	0.100	0.393	0.250	0.141	0.560
La	-0.399	0.599	0.011	0.754	0.588	0.414	-0.117	0.343	0.563	0.073	0.462
Li	-0.153	0.215	0.074	0.217	0.289	0.116	0.310	0.240	0.183	0.219	0.484
Mg	0.163	0.146	0.073	-0.056	-0.124	-0.005	0.485	-0.146	0.130	-0.016	-0.314
Mn	-0.101	-0.076	-0.041	0.014	0.074	0.107	0.088	0.079	0.091	0.486	0.295
Mo	-0.130	-0.054	-0.032	0.041	0.169	0.285	0.180	0.063	0.158	0.431	0.252
Na	0.628	-0.097	0.035	-0.202	-0.334	-0.212	0.450	-0.220	0.010	-0.252	-0.127
Nb	-0.319	0.907	0.011	0.818	0.711	0.490	-0.108	0.470	0.370	0.114	0.312
Ni	-0.194	0.062	0.057	0.115	0.225	0.114	0.239	0.162	0.315	0.420	0.305
P	-0.163	-0.154	0.009	-0.106	-0.078	0.111	-0.232	-0.019	-0.154	0.462	-0.170
Pb	-0.004	0.121	-0.017	0.216	0.087	0.078	-0.047	0.011	0.074	0.149	0.073
Rb	-0.527	0.751	0.000	0.820	0.758	0.430	-0.355	0.491	0.282	0.098	0.358
S	-0.022	-0.365	0.008	-0.236	-0.218	-0.165	-0.452	-0.142	-0.269	0.024	-0.275
Sb	-0.057	-0.229	-0.015	-0.065	0.038	-0.048	0.207	0.128	0.097	0.243	0.433
Sc	0.143	-0.237	0.000	-0.230	-0.172	-0.058	0.734	-0.047	0.330	0.231	0.260
Se	-0.096	0.027	-0.009	0.045	0.102	0.074	0.017	0.041	0.101	0.027	0.017
Sn	-0.340	0.602	0.004	0.606	0.616	0.449	0.020	0.395	0.325	0.245	0.394
Sr	1.000	-0.344	0.051	-0.444	-0.504	-0.153	0.307	-0.345	-0.200	-0.117	-0.353
Ta	-0.344	1.000	0.056	0.823	0.706	0.460	-0.139	0.461	0.331	0.061	0.301
Te	0.051	0.056	1.000	0.012	-0.019	-0.006	0.061	0.004	-0.010	0.032	-0.022
Th	-0.444	0.823	0.012	1.000	0.762	0.496	-0.276	0.464	0.406	0.064	0.404
Tl	-0.504	0.706	-0.019	0.762	1.000	0.453	-0.180	0.485	0.324	0.191	0.482
U	-0.153	0.460	-0.006	0.496	0.453	1.000	-0.043	0.248	0.397	0.291	0.187
V	0.307	-0.139	0.061	-0.276	-0.180	-0.043	1.000	-0.087	0.193	0.196	0.080
W	-0.345	0.461	0.004	0.464	0.485	0.248	-0.087	1.000	0.206	0.144	0.333
Y	-0.200	0.331	-0.010	0.406	0.324	0.397	0.193	0.206	1.000	0.149	0.336
Zn	-0.117	0.061	0.032	0.064	0.191	0.291	0.196	0.144	0.149	1.000	0.198
Zr	-0.353	0.301	-0.022	0.404	0.482	0.187	0.080	0.333	0.336	0.198	1.000